



Cite this: *Nanoscale*, 2016, **8**, 2510

Design, synthesis and applications of core–shell, hollow core, and nanorattle multifunctional nanostructures

Ahmed Mohamed El-Toni,^{*a,b} Mohamed A. Habila,^c Joselito Puzon Labis,^{a,d} Zeid A. ALOthman,^c Mansour Alhoshan,^e Ahmed A. Elzatahry^f and Fan Zhang^g

With the evolution of nanoscience and nanotechnology, studies have been focused on manipulating nanoparticle properties through the control of their size, composition, and morphology. As nanomaterial research has progressed, the foremost focus has gradually shifted from synthesis, morphology control, and characterization of properties to the investigation of function and the utility of integrating these materials and chemical sciences with the physical, biological, and medical fields, which therefore necessitates the development of novel materials that are capable of performing multiple tasks and functions. The construction of multifunctional nanomaterials that integrate two or more functions into a single geometry has been achieved through the surface-coating technique, which created a new class of substances designated as core–shell nanoparticles. Core–shell materials have growing and expanding applications due to the multifunctionality that is achieved through the formation of multiple shells as well as the manipulation of core/shell materials. Moreover, core removal from core–shell-based structures offers excellent opportunities to construct multifunctional hollow core architectures that possess huge storage capacities, low densities, and tunable optical properties. Furthermore, the fabrication of nanomaterials that have the combined properties of a core–shell structure with that of a hollow one has resulted in the creation of a new and important class of substances, known as the rattle core–shell nanoparticles, or nanorattles. The design strategies of these new multifunctional nanostructures (core–shell, hollow core, and nanorattle) are discussed in the first part of this review. In the second part, different synthesis and fabrication approaches for multifunctional core–shell, hollow core–shell and rattle core–shell architectures are highlighted. Finally, in the last part of the article, the versatile and diverse applications of these nanoarchitectures in catalysis, energy storage, sensing, and biomedicine are presented.

Received 9th October 2015,
Accepted 22nd December 2015

DOI: 10.1039/c5nr07004j

www.rsc.org/nanoscale

^aKing Abdullah Institute for Nanotechnology, King Saud University, Riyadh 11451, Saudi Arabia. E-mail: aamohammad@ksu.edu.sa, ahmedtoni@yahoo.com

^bCentral Metallurgical Research and Development Institute, CMRDI, Helwan 11421, Cairo, Egypt

^cAdvanced Materials Research Chair, Department of Chemistry, College of Science, King Saud University, Riyadh 11451, Saudi Arabia

^dMath-Physics Dept., Mindanao State University, Fatima, General Santos City 9500, Philippines

^eDepartment of Chemical Engineering, King Saud University, Riyadh 11451, Saudi Arabia

^fMaterials Science and Technology Program, College of Arts and Sciences, Qatar University, P. O. Box 2713, Doha, Qatar

^gDepartment of Chemistry, Shanghai Key Laboratory of Molecular Catalysis and Laboratory of Advanced Materials, Fudan University, Shanghai 200433, People's Republic of China

1. Introduction

Recently, nanoparticles have increasingly gained attention because of their remarkable properties that result from their nano-dimensions. Continuous development in nanoparticle research has been motivated by the search for new applications, performance improvement, and combined nanomaterial functions (*i.e.*, developing multifunctional nanomaterials). One method to accomplish these objectives is through the coating of nanoparticles with one or more layers of other materials that have interesting properties. The surrounding layer is called the shell, and the original nanoparticle is named as the core. It has been discovered that the constructed layer, or shell, can change the function and properties of the original core. In other words, the core can exhibit new chemical or catalytic reactivity with shell formation. In addition, thermal stability or dispersibility can be improved by growing such shells. In fact, novel optical, magnetic and

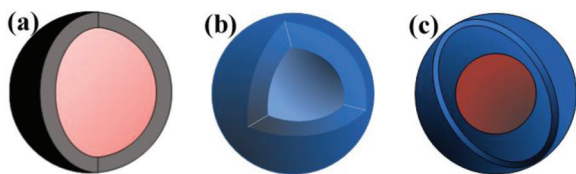


Fig. 1 Multifunctional nanomaterials including (a) core-shell, (b) hollow core-shell, and (c) rattle core-shell nanostructures.

electronic characteristics can be imparted to the core nanoparticle through the formation of a core-shell structure. Therefore, such modified structures could provide the combined functionality of both the core and the shell with novel properties rather than the mono-functionality of nanoparticles alone. This core-shell concept presents two materials with two functions in one structure, as shown in Fig. 1a. By increasing the number of shells and/or the number of materials, the functions of the newly formed structure can consequently be increased, which then offers unlimited possibilities and extensive applications in many fields. For example, a magnetic core can be covered with a porous silica shell that can be loaded with drugs and provide biocompatibility, while the core can simultaneously be used for targeted delivery to a specific organ.¹ Adding an extra shell, or layer, also provides for further functions. For example, an Fe_3O_4 nano-core coated with both a dye-doped mesoporous silica shell and a poly(ethylene glycol) layer can possess tri-functional properties that can be used in magnetic resonance, fluorescence imaging, and drug delivery, thus making it a novel candidate for simultaneous drug delivery and cancer diagnosis.²

However, core-shell structures offer limited storage capacity, and researchers have been seeking more advanced design and geometry modifications to attain more flexibility.

The suitable design and geometry of the core-shell structure allows the formation of other novel architectures, such as hollow core-shell structures (as shown in Fig. 1b) through removal of the core. The large fraction of empty space in the hollow structures has been used as a system for the loading and controlled release of special materials, such as drugs, genes, peptides, and biological molecules.³ The hollow cavity within the sphere can be used as a nanoreactor with catalytically active species loaded for catalytic reactions,⁴ or to tune the refractive index, decrease density, improve particle resistance toward continuous volume change, or to provide imaging markers designed for cancer detection.^{5,6} Furthermore, the hollow cavity is characterized by having a high surface area and pore volume as well as the capability of capturing hazardous materials within their interior void.⁷

Despite the outstanding storage space provided by hollow core structures, one of their main drawbacks is the lack of an internal core. A novel approach to combine the high storage capacity of hollow spheres with the advantages of the core-shell structure is to create one or more cavities between the outer shell and the inner solid core, producing a structure known as the rattle-type or yolk-shell. In other words, the yolk or rattle core-shell architecture (Fig. 1c) could be described as having a core@void@shell configuration.⁸ The rattle structure possesses the combined properties of the solid cores, such as magnetic, metal, or quantum dot nanoparticles, together with those of the void in-between the core and the shell, which can be used for extra storage. Rattle core-shell multifunctional nanomaterials have gained considerable attention in recent years and have shown promising applications as nanoreactors, drug/gene delivery agents and lithium-ion batteries.⁹⁻¹⁴

In this review, a comprehensive overview of the multifunctional core-shell, hollow core, and nanorattle nanoarchitectures is presented. Further highlights are focused on the emerging



Ahmed Mohamed El-Toni

Ahmed Mohamed El-Toni received his Ph.D. in 2006 from the Institute of Multidisciplinary Research for Advanced Materials, Tohoku University (Japan). In 2007, he joined the Functional Assembly Technology group, the National Institute of Advanced Industrial Science and Technology (AIST), Nagoya (Japan) as a research fellow. Then by 2008, he joined King Abdullah Institute for Nanotechnology (KAIN), King Saud

University, Riyadh, Saudi Arabia. Currently, he holds the position of an associate professor in KAIN and his research interests include the synthesis of novel core-shell multifunctional nanomaterials and their application into drug delivery, enzyme immobilization and water treatment.



Mohamed A. Habila

Mohamed Habila has received his Ph.D. in 2015 from the chemistry department, King Saud University, Riyadh, Saudi Arabia. Currently he is an assistant professor in the advanced materials research chair, chemistry department, King Saud University. His research interests include fabrication of multifunctional core-shell nanomaterials for separation and pre-concentration techniques, wastewater treatment as well as carbon based materials for hydrogen storage applications.

trends of their prospective designs, synthesis approaches, and applications. This article is organized as follows. In the first section, different design strategies for the core-shell, hollow core, and nanorattle multifunctional nanostructures are discussed. In the second section, the key synthesis approaches for constructing each of these nanostructures are summarized. In the third section, a range of potential applications of core-shell, hollow core, and nanorattle multifunctional nanostructures, including nanocatalysis, biomedical applications, lithium-ion batteries and sensing fields, is reviewed.

2. Design of multifunctional nanomaterials

2.1. Core-shell

Nanoparticles have received more research attention than bulk materials due to their superior properties; however, from the beginning of the 1980s, studies have been concentrated on composite nanomaterials that include more than one particle because they exhibited new and improved properties.^{15–17} By the end of the 1990s, multilayer composite nanoparticles had been developed and showed significantly improved performance due to their structure.^{18–20} By this time, the term core-shell nanoparticles had become more common, and many investigations and studies had been directed toward to this novel branch of materials.

The core-shell structures are composite materials that contain an inner core coated with one or more layers (shells) of different materials. The materials of the core-shell structures can exist in different combinations,²¹ such as core and shell materials that are organic or inorganic. Furthermore, organic cores can be coated with inorganic shells and *vice versa*.²¹ The physical and chemical properties of core-shell nanoparticles are mainly associated with the materials and structure of the core and shell, but they are also associated with the interface. This structure dependence provides huge

opportunities and possibilities for manipulating properties by controlling the chemical compositions and relative sizes of the core and shell.^{22,23}

The selection of the core and shell material is related to the type of targeted application. Therefore, design of multifunctional core-shell nanoparticles usually depends on the final application. For drug delivery, the core material could possess magnetic characteristics, and the outer shell could be a polymer or porous silica.²⁴ Similarly, for separable nanocatalysts, the core material can be Fe_3O_4 or Fe_2O_3 , while the shell could be a metal nanocluster.²⁵ For stable nanocatalysts,²⁶ Pt metal nanoparticles can be stabilized from growing in size, by the effect of high temperature, through coating them with a porous silica shell that allows the diffusion of the reactants and products through the shell. In this architecture, the morphology, size and stability of metal cores can be maintained regardless the working temperature. For designing a system capable of performing photothermal/chemotherapy and multimodal imaging of cancer,²⁷ the magnetic core, which is responsible for multimodal imaging capability, can be coated with a porous silica layer in which chemotherapy drug molecules can be encapsulated. Finally, gold nanorods can be formed as a second shell around the mesoporous silica shell, and these can function as photothermal therapeutic agents.

In fact, core-shell structure design can also be affected by the core type and size. For a multifunctional, multimodal imaging core-shell system, upconversion nanoparticles can be used as the shell material, while Fe_3O_4 nanoparticles can be used as the core for magnetic resonance imaging applications. The selection of a suitable core size is crucial to design an efficient core-shell system; the appropriate magnetic core size for drug delivery applications is between 50 and 300 nm. Nanoparticles larger than 300 nm will be trapped in the lungs and liver, while nanoparticles smaller than 50 nm will possess magnetic forces too weak for drug delivery.²⁸ Functionalization of the core surface with organic functionalities can be considered as an important step for constructing/designing the outer shell. To fabricate a gold shell around the magnetic/silica cores, the core surface should contain thiol groups as functional moieties that can be attached to gold nanoclusters for shell formation.²⁹

These design concepts can also be extended to the tuning of core and shell physical characteristics, *i.e.*, from dense to porous, by using surfactant molecules.³⁰ Various spherical core/shell nanoarchitectures can be constructed based on the nature of the core and shell materials; cores can be dense (solid) or porous (Fig. 2a). Moreover, different types of shells are possible, such as continuous/discontinuous dense shells, continuous porous shells (Fig. 2a), and multiple shells (Fig. 2b).³¹ In addition, other designs can be created by choosing core materials of different shapes. In addition to the usual spherical morphology of core-shell nanoparticles, there are many other possible shapes of core/shell nanoarchitectures, depending on the various core morphologies that are available, including nanorods, nanotubes, nanowires, nanorings and nanostars.^{21,32–36}



Joselito Puzon Labis

Joselito Puzon Labis received his Ph.D. from the Division of Quantum Materials Physics, Graduate School of Natural Science and Technology, Okayama University, Japan in 2002. Then, he joined as a research fellow at the Hiroshima Synchrotron Radiation Center, Hiroshima University, Japan. In 2010, he was appointed as an assistant professor at the King Abdullah Institute for Nanotechnology, King Saud University,

Riyadh, Saudi Arabia. His current research focuses on the nanostructures of III–V materials and ZnO for solar cells and other applications.

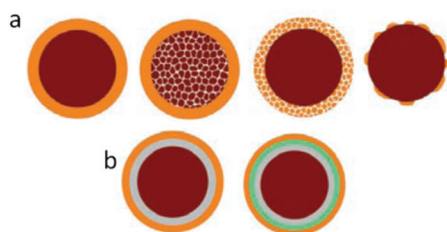


Fig. 2 Designs to produce different core-shell architectures with (a) different porous core and shell characters, (b) different core-multiple shell structures. (Reprinted with permission from the Faculty of Technology, University of Novi Sad.)³¹

2.2. Hollow core-shell

Over the past few decades, interest in monodisperse hollow spheres has grown considerably in response to their unique properties, such as uniform size, well-defined morphology, large surface area, low density, and wide range of potential applications. Such applications make use of the large empty cavity in these hollow structures, which can be used for the loading and controlled release of specific molecules, such as drugs, peptides and genes.^{3,5} In addition, hollow core spheres are used as refractive index modulators; other usages include increasing the active catalysis area and hence its adsorption, lowering the particle density, expanding the array of imaging markers that can be used in early cancer detection, and improving particle tolerance to cyclical volume changes.^{6,37} Due to their special optical, thermal, catalytic, electro-chemical, photo-electrochemical and mechanical properties, inorganic hollow spheres could comprise a more diverse and richer class of materials than organic hollow core spheres.³⁸

The hollow sphere concept arose when there was a need for lowering the nanoparticle density or constructing nanoparticles with huge storage capacities together with enhanced capture capabilities. The design of the hollow core spheres was first initiated by the concept of core removal, or the hard templating approach.³ This process involved the removal of different types of core materials, such as metals,³⁹ metal oxides,⁴⁰ and polymer nanoparticles.⁴¹ Designing hollow core-shell nanostructures also includes tuning their size and shape. Size tuning can be performed by the precise selection of the core size prior to the core removal step.

Shape tuning has been conducted by selecting core templates of different morphologies to obtain hollow spheres,⁴² hollow nanocubes,⁴³ hollow fibers,⁴⁴ and hollow nanoplates.⁴⁵ Furthermore, variation of the hollow nanoparticle composition has been performed by choosing suitable shell materials, which can include metals,⁴⁶ metal oxides,⁴⁷ and polymers.⁴⁸ Moreover, the shells of hollow nanoparticles can be solid with a dense character, similar to most polymer and metal shells,⁴⁹ or they can be made porous by the addition of surfactant molecules during shell formation, as is the case with many metal oxide shells.⁵⁰ In addition, controlling the number of shells (single,⁵¹ double,⁵² or multiple⁵³) can be another tool for designing hollow core-shell multifunctional nanomaterials.

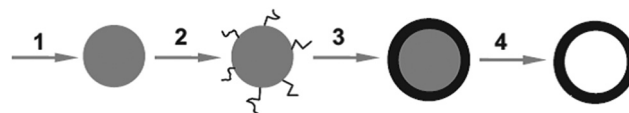


Fig. 3 Schematic illustration of a conventional hard templating process for hollow sphere synthesis. (Reprinted with permission from John Wiley and Sons.)⁹

The template method, in particular, is the most common method for producing hollow core-shell structures. In this method, there are usually at least two steps that are indispensable. First, the templates must be modified such that they will have the ability to attract inorganic precursors (salts or alkoxides) onto the surface of the template core. Next, after the decoration of the inorganic shell, the templates are eliminated, which results in the hollow core-shell formation (Fig. 3).^{3,9}

Generally, we can categorize the templates as hard or soft. When using hard templates, such as SiO₂,⁵⁴ carbon,⁵⁵ polymers,^{56,57} and metals,⁵⁸ the resulting hollow product will have a structure similar to that of the template and will exhibit a well-defined and monodisperse morphology. However, removing the templates by thermal (sintering) or chemical (etching) means can be a very complicated and energy-consuming procedure. Soft templates, such as bacteria,⁵⁹ droplets,⁶⁰ and vesicles,⁶¹ are easier to remove; however, both the morphology and the monodispersity of the resulting hollow nanoparticles are usually poor due to the deformability of the soft template. Nevertheless, although the drawbacks of these templating approaches may seem inherent and insurmountable, novel emerging techniques, *e.g.*, sacrificial templates and modified soft templates, may have the potential to overcome these disadvantages.³

2.3. Rattle core-shell structure

The demand for combining the functional properties of the core-shell structure with the huge storage capacity of the hollow core-shell structure has led to the construction of a novel rattle core-shell system, which exhibits the merits of both architectures. Nanorattles represent a new and novel class of special core/shell structures with a characteristic core@void@shell configuration (Fig. 4a).⁶² Among complex multifunctional nanoarchitectures, the rattle core-shell nanomaterials (also known as “yolk/shell” structures, where the nanoparticle core is contained by one or more hollow shells)

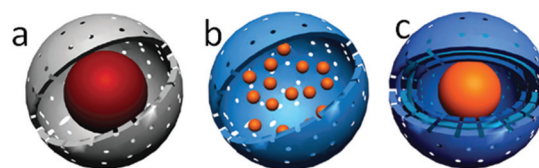


Fig. 4 Designs to produce the different nanorattle architectures of (a) core-shell, (b) multiple-core and (c) multiple-shell. (Reprinted with permission from the Royal Society of Chemistry.)⁶²

have attracted a great deal of attention due to their appealing structures, tunable physical and chemical properties. The tailor-ability and functionality of both the cores and hollow shells also make nanorattles promising for a range of remarkable applications, such as catalysis, biosensors and surface-enhanced Raman scattering.^{9–14}

Over the last two decades, research on these functionalized nanorattle materials has been geared towards the design and fabrication of different morphologies for desirable properties.^{9,10} Recently, catalytically active systems designed using nanorattle architectures with metal cores such as Au, Ag, Pt, and Ni showed outstanding performance for various catalytic reactions.^{14,63,64} The nanorattle catalysts provide high activities that are attributed to the freely moving core within the protective shell (Fig. 1). This configuration offers a homogeneous environment for heterogeneous catalytic activities.^{11–14,65,66–68} Since Au@polymer nanorattles were first reported by Xia *et al.*, a number of nanorattles with different core-shell configurations and compositions with different sizes and shapes have been developed.^{8–13,69–71}

Furthermore, nanorattles have been engineered and designed over a wide range of chemical compositions, including metal@polymer,⁶⁵ metal oxide@silica,⁶⁶ metal@carbon,⁶⁷ metal@silica,⁶⁸ polymer@polymer,⁶⁹ silica@metal oxide,⁷⁰ metal@metal oxide,⁷¹ and metal silica@carbon.⁷² In addition, multiple-core nanorattles (Fig. 4b) and multiple-shell nanorattles (Fig. 4c) have also been recently designed and studied. Driven by the interesting compositions and tailored properties, novel fabrication methods have been developed to functionalize these unique nanorattles. As a result, nanorattles can be produced by many techniques, such as the selective-etching, galvanic replacement, soft-templating, Ostwald ripening and ship-in-bottle approaches.

For example, the catalytic activity of metal nanoparticle@silica nanorattle catalysts is significantly enhanced by their unique design, where each metal nanoparticle core is prevented from aggregating by the outer protective shell. Moreover, these cores are movable, which allows them to possess more exposed active sites.^{12–14,67} Additionally, the diffusion rates of the reactants are controlled by manipulating the structure of the core and the porosity of the shell, and consequently the confined reaction environment becomes quite similar to that of homogeneous catalysis.^{72–74}

Furthermore, rattle core-shell nanoparticles present a new and novel platform for investigating the cooperative effects of the two catalysts in a rattle structure.⁷⁵ It is worth mentioning that the large hollow space between the core and the shell in nanorattles can be designed to accommodate fluorophores or drug molecules. They can then function as promising delivery vehicles for targeted drug/gene delivery research.^{76–78} In addition, the voids in the rattle-core/shell structure can be engineered to be exploited as a buffering space for the electroactive core materials in a lithium insertion–deinsertion process to improve the cycling performance of electrode materials. Therefore, nanorattles are very promising materials for lithium-ion battery research.^{1,79,80}

3. Routes for fabrication of different multifunctional nanomaterials

3.1. Core-shell nanomaterial fabrication

3.1.1. Core materials. Attaining the final applications and targeted properties of core-shell nanoparticles is mostly dependent on careful selection of both the core and shell materials. The core can be composed of various metals, metal oxides, quantum dots, and polymer materials. Many investigations have been directed toward constructing core-shell systems based on metal oxides,^{81,82} noble Au^{83,84} and Ag,^{85,86} non-noble Ni,⁸⁷ Co,⁸⁸ and Fe,⁸⁹ and polymer nanocores.^{90,91}

Metal oxide nanoparticles have been used as core materials for photocatalytic, drug control release and drug delivery applications. Additionally, noble metal nanocores have been used for nanocatalysis as well as photothermal cancer therapy. Quantum dots have been used as cores for bio-imaging and diagnostic applications. Iron, nickel, cobalt, manganese, chromium and gadolinium⁹² nanocores have gained attention because they play important roles in magnetic resonance imaging as well as separation technology.⁹³ Moreover, iron oxide nanoparticles have also been a promising multifunctional nanosystem for imaging and therapy; they have unique properties, such as biocompatibility, an intrinsic ability to enhance magnetic resonance contrast, and facile surface modification, and therefore they are excellent theranostic agent candidates.^{93,94}

3.1.2. Shell fabrication. Several approaches have been established to construct a protective layer or shell around different types of nanoparticle cores. In all of these methods, the cores are formed first, and then shell formation takes place. The core surfaces provide nucleation sites (seeds) for the shell atoms to nucleate and grow through sol-gel or chemical precipitation approaches. In other words, the core acts as a substrate for shell deposition. Different types of shell materials require different coating or shell formation strategies.

3.1.2.1. Metal oxide shell. Metal oxide is a class of materials that possess a wide spectrum of properties. Upon depositing a metal oxide layer on another type of nanoparticle, a combination of properties can be obtained. For example, metal oxide coatings can endow iron oxide nanoparticles with interesting semiconducting and magneto-optical properties. For instance, iron oxide nanoparticles can be utilized for the selective enrichment of phosphopeptides by coating them with Al₂O₃,⁹⁵ ZrO₂,⁹⁶ TiO₂,⁹⁷ and Ta₂O₅⁹⁸ metal oxide shells.

However, despite the various types of metal oxides being used as a coating layer, SiO₂ is still most common for shell formation. The well-established synthesis route used to prepare nanoparticle@SiO₂ core-shell nanostructures is the sol-gel approach, which involves hydrolysis and condensation of the silica precursor (tetraethyl orthosilicate). The sol-gel approach has been implemented for the coating of noble metal nanocores with silica shells, such as Au@SiO₂,⁹⁹ Ag@SiO₂¹⁰⁰ (Fig. 5a), and Pd@SiO₂.¹⁰¹ The silica coating is so commonly used because of its amorphous character and facile shell formation process.

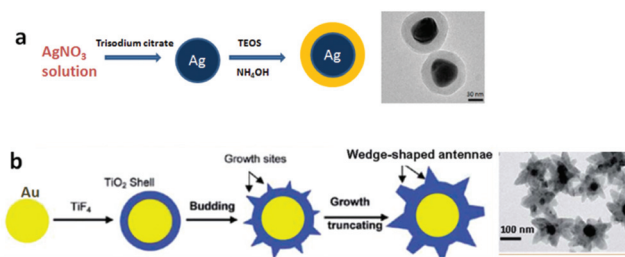


Fig. 5 Scheme of the proposed formation process and TEM images of (a) a SiO₂ shell around a Ag nanocore, (Reprinted with permission from the American Chemical Society.)¹⁰⁰ and (b) a TiO₂ shell around an Au nanocore. (Reprinted with permission from the Royal Society of Chemistry.)¹⁰⁷

However, upon growing other crystalline metal oxide shells such as TiO₂ on the surface of nanoparticle cores, especially metallic cores, self-nucleation and uncontrollable growth takes place due to large interfacial stress between the shell and metallic nanocores. Nevertheless, this issue can be resolved by the addition of surfactant molecules to prompt nucleation and growth of the metal oxide shell around the metal nanocore. Using this concept, TiO₂ shells have been coated around Au nanoparticles¹⁰² through the addition of hydroxypropyl cellulose to modify citrate-stabilized Au nanoparticles. Thereafter, the less reactive sol-gel precursor titanium diisopropoxide bis(acetylacetonate) can be used to create TiO₂ shells around Au nanocores. However, titanium tetrabutoxide showed much lower hydrolysis compared with titanium diisopropoxide, which indicates that butoxide is a more suitable precursor for homogeneous TiO₂ shell formation. Fornasiero *et al.* constructed Pd@CeO₂ core-shell nanostructures by utilizing the self-assembly between the functionalized Pd nanoparticles and cerium alkoxides.^{103,104}

Another method that can be used for fabrication of metal oxide shells instead of the sol-gel technique is the hydrothermal process. The hydrothermal process has many advantages, such as being non-toxic and environmentally friendly and having low cost, solubility with a broad range of materials, and polar affinity, which facilitates the controlled growth of metal oxide shells.¹⁰⁵

Generally, the hydrothermal method is conducted within a sealed vessel, where the water creates pressure upon heating and helps to improve the crystallinity of the prepared nanoparticles. Zhang *et al.* have used the hydrothermal method to grow CeO₂ shells around Pt cores. In this work, CeCl₃ and citrate-stabilized Pt were mixed in the presence of urea (at desired concentrations) and heated in an autoclave at 90 °C for desired times.¹⁰⁶

In comparison with the sol-gel process, the hydrothermal process does not require the use of surfactants to facilitate metal oxide shell formation. Moreover, the simplicity and environmental friendliness of the hydrothermal method support its expansion as a shell construction method. However, a deeper understanding of the process is required for

controlling the heterogeneous nucleation and growth of metal oxides on metal nanocores rather than forming metal oxide nanoparticles (Fig. 5b).¹⁰⁷

3.1.2.2. Metal shells. Coating nanoparticle cores with noble metal shells has become an attractive research topic because it is expected to provide novel characteristics and versatile applications. One of the most important methods for constructing noble metal shells is the reverse micelle approach, which serves as a nanoreactor for shell growth by adjusting the ratio of the metal salt to the reducing agent. This method has been implemented to grow metal shells around Co and Fe nanoparticles.^{85,108–111}

Another method that has been extensively utilized for the synthesis of metal shells is the thermal decomposition method for organometallic precursors.^{111,112} For coating a Pd shell around a Ni Core, Ni(acac)₂ and Pd(acac)₂ were added to oleylamine at an elevated temperature.¹¹² Knowing that the Ni-TOP complex tended to decompose faster at a lower temperature than the Pd-TOP complex, while the Pd-TOP complex tended to decompose more easily at higher temperatures than the Ni-TOP complex; then by performing the thermal decomposition reaction at a lower temperature (205 °C) Ni cores can be formed easily, while the Pd-TOP complex maintains its stability. By elevating the reaction temperature to 235 °C, the Pd-TOP complex begins to decompose and form a Pd shell around the previously formed Ni cores.¹¹²

To fabricate metal shells on magnetic nanoparticles, thermal decomposition methods have also been utilized. However, Fe₃O₄ nanoparticles were first synthesized by the decomposition of iron(III) oleate into a mixture of oleic acid and oleylamine. Thereafter, an Au shell was introduced to the Fe₃O₄ surface by HAuCl₄ reduction in the oleylamine and chloroform mixture. The Au-Fe₃O₄ core-shell nanoparticles could then be transferred to the water solution by adsorbing cetyltrimethylammonium bromide (CTAB) and sodium citrate to make them more hydrophilic for facile mixing with water. Thereafter, the Au shells surrounding the Fe₃O₄ cores could be grown thicker by dispersing the hydrophilic Fe₃O₄-Au into water with the addition of HAuCl₄ and a reducing agent. Furthermore, a second Ag shell also could be constructed around the Fe₃O₄@Au core-shell nanoparticles by adding AgNO₃ with the reducing agent. It is worth mentioning that the plasmonic properties of the core-shell nanoparticles can be tuned towards blue shift (approximately 501 nm) or red shift around (560 nm) (Fig. 6). Fe₃O₄@Au core-shell nanoparticles offer not only the double functionality of the magnetic character and plasmonic properties but also long-term for core and shell material stability. It is expected that Fe₃O₄@Au core-shell can possess great opportunities for therapeutic and diagnostic applications.¹¹³

3.1.2.3. Dense shells. Most of the shells formed around different types of cores are dense, or solid. The dense shell implies that no pores exist in its structure. The dense shell is usually a metal oxide such as alumina or silica, and can also be a non-metal such as carbon. The shell material types determine the final character of core-shell nanoparticles. When

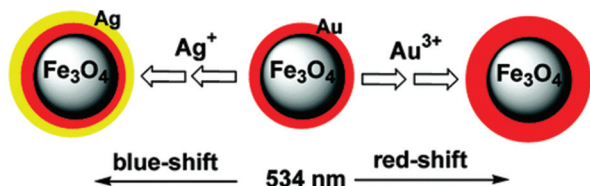


Fig. 6 Scheme diagram for tuning the plasmonic properties of the magnetic core–metal shell nanoparticles by controlling the shell type and thickness. (Reprinted with permission from the American Chemical Society.)¹¹³

silica or alumina is selected as a shell material, the final core–shell will show a hydrophilic character; however, when carbon is used as an outer shell, the final core–shell nanoparticles will show a hydrophobic character. Silica and carbon are the most common dense shell materials that have been used for insulating/protecting magnetic nanoparticles from oxidation/dissolution.

The magnetic core–dense shell structure can be utilized with biological samples through chemical bonding or physical adsorption. Dense silica shells have been coated onto different types of cores using the Stöber method. In this process, the silica precursor (TEOS) is hydrolyzed under alkaline conditions to form silica nuclei that can be seeded on the surface of the nanoparticle cores in a heterogeneous nucleation step. Thereafter, in the growth step, the newly formed silica nuclei begin to bond to the previously formed silica seeds to produce a homogeneous shell. The nucleation and growth steps can be controlled by manipulating the TEOS and alkali (NaOH, NH₄OH) concentrations. The shell thickness can be controlled by increasing the TEOS concentration or prolonging the reaction time.

A similar strategy can be extended to alumina or titania shells. It is worth mentioning that silica shells will not be affected by heat treatment due to their amorphous character. However, titania and other crystalline shells will undergo grain growth due to a phase change from amorphous to crystalline, which may result in a loss of the dense shell character. The carbon shell can be grown on the surface of core nanoparticles by high temperature processes such as the chemical vapor deposition (CVD) method. Wet processes such as the hydrothermal and solvothermal methods can be used to carbonize glucose material to form protective carbon shells. However, in recent years, polymer shells that can be coated more homogeneously around the core nanoparticles have been found to be more suitable candidates for forming carbon shells through a carbonization step.^{3,9}

3.1.2.4. Mesoporous shells. As mentioned before, dense shells have been constructed with the aims of protecting, insulating and providing multi-functionality. However, turning a dense shell into a mesoporous one can provide new opportunities because such shells can accommodate molecules and allow the diffusion of materials into and out of the core. A mesoporous shell is a shell exhibiting pores with diameters

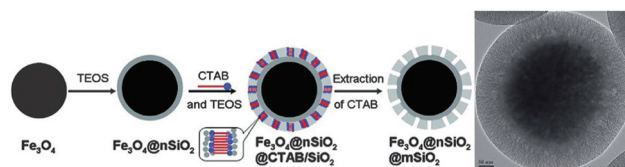


Fig. 7 The formation and a typical TEM image of Fe₃O₄–*n*SiO₂@mSiO₂ microspheres. (Reprinted with permission from the American Chemical Society.)¹¹⁵

ranging from 2 to 15 nm, depending on the type of the pore forming agent (surfactant) used. In addition, the mesoporous shell has advantages over the dense shell due to its chemical composition and textural properties associated with their high shell pore volumes.

The mesoporous silica shell was first reported by Büchel *et al.* in 1998; their process of *n*-octadecyltrimethoxysilane (C₁₈TMS) hydrolysis did not use a surfactant and resulted in the formation of non-ordered mesoporous shells.¹¹⁴ Zhao *et al.* have used a cationic surfactant (Cetyl trimethylammonium bromide) to form ordered, perpendicularly aligned mesoporous SiO₂ shells around magnetic nanoparticles cores, as shown in Fig. 7.¹¹⁵ Thereafter, many studies have implemented cationic surfactants as tools for the construction of ordered mesoporous silica shells around different types of cores. In addition, El-Toni *et al.* have reported amino-functionalized mesoporous shell fabrication around silica cores,¹¹⁶ and magnetic¹¹⁷ nanoparticles using anionic surfactants. Mesoporous silica shells with large pore sizes (7 nm) have also been formed by using a copolymer (Plunoric P123) surfactant.¹¹⁸ The selective-etching method has also been used to convert dense silica shells into non-ordered mesoporous shells, as reported by Ge *et al.*¹¹⁹ In this method, silica shells were stabilized by the adsorption of polyvinylpyrrolidone (PVP) molecules, and an alkaline etchant was then introduced to form pores within the shells.

3.2. Hollow structure fabrication

3.2.1. Hollow core–shell nanomaterial fabrication. Hollow core–shell nanostructures are usually fabricated by first synthesizing the core nanoparticle and then coating the shell materials onto the cores. Thereafter, removal of the core materials results in hollow core–shell structure formation. This process is usually designated as hard templating and can include polymers, metals, and metal oxide cores as hard templates. However, the other common process for hollow core–shell structure fabrication is the soft templating process that is based on utilizing shell material precursors together with surfactant molecules under special conditions to form hollow core–shell structures. The following sections will discuss both the approaches.

3.2.2. Hard template strategy. Different types of templates, including polymers, metals and metal oxides, have been implemented for the fabrication of hollow core structures. The

final size of hollow core nanoparticles can be controlled by adjusting the size of the template.

3.2.2.1. Polymer template-based methods. Polymer nanoparticles can be considered as the most commonly used hard template for producing hollow spheres. The polymer templating method can be classified into two main categories. The first category includes methods based on the usage of polymer beads, such as polystyrene nanoparticles and their derivatives, to construct hollow spheres of SnO_2 ,¹²⁰ SiO_2 ,¹²¹ Fe_3O_4 , Co_3O_4 and $\text{Ni}(\text{OH})_2$.¹²² The shells are formed on the polystyrene nanoparticles either by surface reaction based on the functional groups present on the core surface or by controlled precipitation of inorganic metal salt molecules. To obtain the hollow structures, polystyrene nanoparticles are removed by either calcination processes in air or by selective dissolution using a suitable solvent. Hollow silica spheres have been prepared by synthesis with polystyrene nanoparticles.¹²⁴ The silica shell was coated on the polystyrene cores *via* condensation between silanol groups on the core surface and the silica precursor (TEOS) through the alkaline catalyzed sol-gel method. By calcination at 600 °C, the polystyrene cores were decomposed, and hollow core silica spheres were formed.¹²³

Hollow TiO_2 spheres have also been synthesized using sulfonated polystyrene nanoparticles. The existence of sulfonate groups improves the hydrophilic character of polystyrene nanoparticles and allows interaction with shell precursors such as titanium butoxide, producing hollow titania spheres. Upon addition of titanium butoxide to the solution of sulfonate functionalized polystyrene nanoparticles, hydrolysis begins to form the TiO_2 shells. Finally, by the solvent dissolution of the polystyrene cores, hollow titania spheres can be obtained.¹²⁴

The second category includes methods of layer-by-layer self-assembly.^{125,126} The layer-by-layer technique is based on the electrostatic attraction of oppositely charged species that have been alternately deposited on polymer nanoparticles. In this approach, multilayered shells are formed on the polystyrene nanoparticles through the adsorption of the polyelectrolyte and oppositely charged nanoparticles. Uniform hollow spheres of different types of inorganic materials, including Mn_2O_3 ,¹²⁷ SiO_2 ,¹²⁵ and TiO_2 ,¹²⁸ have been produced by performing the calcinations of the formed core-shells to remove the polystyrene cores as well as the polyelectrolyte (Fig. 8).

It is worth mentioning that this method is conducive for controlling the hollow sphere diameter and shell thickness by allowing the adjustment of polystyrene nanoparticle size and inorganic precursor concentration, respectively.

The advantages of polymer-based templating methods include the ability to produce hollow spheres of metals, metal oxides and non-metal nanoparticles with variable cavity diameters, shell thicknesses, and surface functionalities. However, the time and energy consumption required for this method are disadvantageous. The time consumption is due to the need for multiple steps to obtain the hollow sphere structure, such as the preparation of the core nanoparticles, the coating process, the adsorption of polyelectrolyte, and the multiple separation and washing steps. Moreover, energy consumption

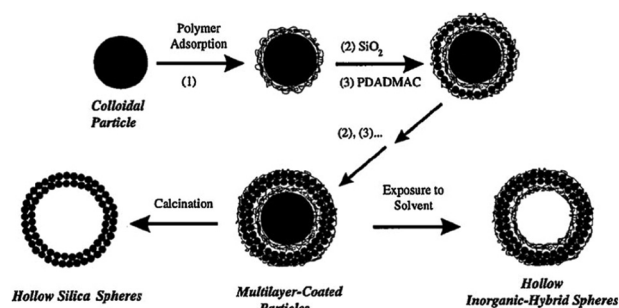


Fig. 8 Schematic illustration of procedures for preparing inorganic and hybrid hollow spheres using the layer-by-layer (LBL) technique based on PS colloidal templates. (Reprinted with permission from The American Association for the Advancement of Science.)¹²⁶

comes from the calcination processes that require elevated temperature conditions.³

3.2.2.2. Inorganic non-metallic template-based methods. Carbon and silica have been used as non-metallic templates for the synthesis of hollow core nanoparticles.³ Easy removal of carbon nanoparticles as well as their multiple and numerous reactive groups support their suitability for the templating process. Various metal oxide hollow spheres, including MnO_2 , Ga_2O_3 and NiO ,^{129–131} have been fabricated through the carbon templating process using carbonaceous polysaccharide spheres.³ Upon hydrothermal treatment of carbonaceous polysaccharide, carbon spheres are formed that are hydrophilic in nature due to the presence of hydroxyl groups. These groups can bind metal cations easily during the shell formation step through electrostatic attraction or coordination. By performing calcinations, the metal salts forming the shell are condensed and cross-linked together to form a metal oxide layer, while the carbon cores are thermally decomposed to produce hollow structures. Based on the carbon templating method, Liu *et al.* have prepared 300 nm hollow Gd_2O_3 : Ln (Ln = Eu^{3+} , Sm^{3+}) microspheres,¹³⁰ where glucose under hydrothermal conditions forms carbon spheres containing hydroxyl groups. During the coating step, Gd^{3+} and Ln^{3+} precipitate in the presence of urea onto the carbon spheres, and by calcinations at 300 °C, the hollow spheres are formed. Co_3O_4 , CeO_2 , Fe_2O_3 , Ni_2O_3 and CuO hollow core spheres¹³² have also been formed by a one-pot hydrothermal method by mixing carbohydrates and metal salts and then heating them in an autoclave at 180 °C. Using such methods, a wide range of metal oxide hollow spheres that were not accessible *via* the sol-gel approach have been synthesized. The surface area and thickness of the shells can be tuned by controlling the carbohydrate : metal-salt ratio.¹³¹

3.2.3. Soft template-based strategies. The soft templating method represents an attractive research track for synthesizing hollow structures because the templates can be removed in a simple and easy way.^{132–136} However, the main disadvantages of soft templating methods are the poor monodispersity and lack of control over particle morphology, which can be

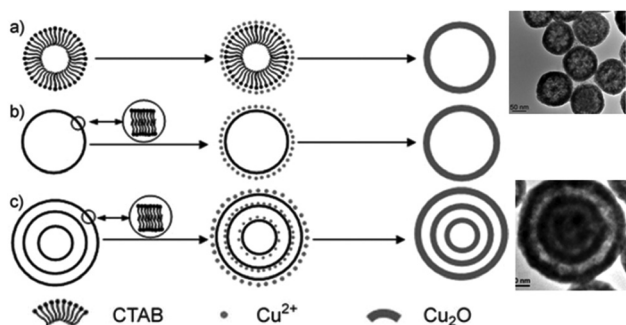


Fig. 9 The formation of different Cu_2O hollow structures in the presence of a CTAB template: (a) micelle, (b) single-lamellar vesicle, (c) multi-lamellar vesicle. (Reprinted with permission from John Wiley and Sons.)¹³⁵

attributed to soft template deformation. Therefore, the most challenging aspect is the fabrication of uniform and monodisperse hollow spheres. In this regard, 11–30 nm $\text{La}(\text{OH})_3$ hollow spheres have been reported by Leidinger *et al.*¹³⁷ through construction of W/O microemulsion using *n*-dodecane as the nonpolar oil phase, Cetyl trimethylammonium bromide as a surfactant and 1-hexanol as a co-surfactant. Monodisperse micrometer-sized SiO_2 hollow spheres have been fabricated, where the outer and inner diameters of the hollow spheres could be controlled by adjusting the water to the surfactant ratio of the underlying micellar system, which, in turn, affected the size of the relevant micelles and influenced the outer diameter and cavity size. Multi-shelled Cu_2O hollow spheres with a single-crystalline shell wall have been prepared using a soft templating method as shown in Fig. 9.¹³⁵ Furthermore, 50 nm silver spheres having wall thicknesses of 3–5 nm and 10–15 nm diameter inner cavities were also obtained by implementing a soft templating approach.¹³⁸ In addition, further complex hollow cage-like silica spheres loaded with iron oxide nanoparticles in their porous shells have been fabricated using the oil-in-diethylene-glycol microemulsion approach.¹³⁹ Zoldesi *et al.* have prepared monodisperse SiO_2 hollow spheres using polydimethylsiloxane (PDMS) silicone O/W emulsion templating.¹⁴⁰

3.3. Rattle core-shell nanomaterial fabrication

Rattle core-shell nanostructures can be fabricated using five main approaches: selective-etching, soft templating assembly, ship-in-bottle, Ostwald ripening, and galvanic replacement. Furthermore, in some cases, combinations of these approaches have been used to construct rattle core-shell nanostructures with high degrees of functionality and complexity.

3.3.1. Selective-etching or dissolution methods. Recently, the selective-etching approach has been considered an important tool for fabricating rattle core-shell nanoparticles. In this process, the core nanoparticles are coated with double shells of two different materials. Thereafter, the intermediate shell is selectively etched by a suitable solvent or by calcination steps to construct the rattle structure (Fig. 10). In some cases, the

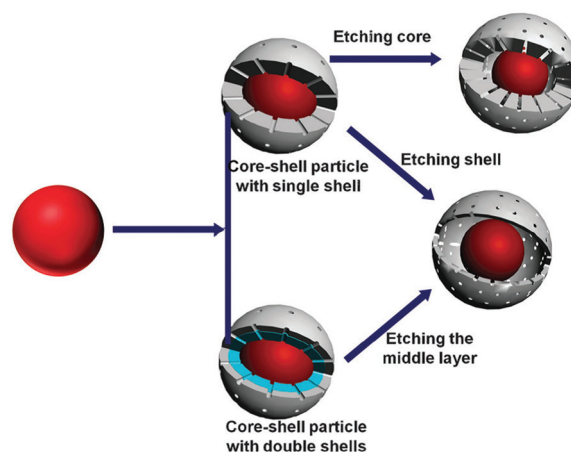


Fig. 10 Schematic illustration of etching strategies for preparing rattle core-shell nanoparticles. (Reprinted with permission from the Royal Society of Chemistry.)⁶²

cores are coated with one shell, and then either the inner part of the shell or the outer part of the core is dissolved to produce the targeted structure. The selective-etching approach has been implemented to fabricate rattle core-shell nanostructures with a spherical morphology as well as non-spherical rattle nanostructures such as ellipsoids and ‘sword-in-sheath’ architectures.^{72,141–143}

3.3.1.1. Partial removal of the core or the shell. This method is based on the selective removal of the outer part of the core, the inner part of the shell, or the intermediate shell at the core-shell or core-double shell structure through using a suitable solvent or calcination step (Fig. 10).⁶² Based on this approach, a three-layered ‘sandwich’ structure of organic-inorganic hybrid solid silica spheres has been synthesized, first by the hydrolysis of TEOS and N-3-(trimethoxysilyl)propylethylenediamine, producing silica spheres containing an organosilica layer.¹⁴⁴ Thereafter, the rattle nanostructure was obtained by selectively etching the middle organosilica layer using specific amounts of hydrofluoric acid.

$\text{Fe}_3\text{O}_4@/\text{SiO}_2$ rattle core-shell nanostructures with inner cavities have been fabricated by forming carbon spheres around the magnetic nanoparticles in a one-pot hydrothermal method using carbon and iron precursors. Thereafter, silica shells were formed around the carbon-coated magnetic nanoparticles. $\text{Fe}_3\text{O}_4\text{-SiO}_2$ rattle nanostructures were finally obtained through carbon removal by a calcination process.¹⁴⁵ Using cross-linked polymethylmethacrylate (PMMA) as a middle or intermediate layer between two different types of inorganic materials, such as $\text{TiO}_2@/\text{SiO}_2$, with subsequent sample calcination, corresponding rattle nanostructures have been formed.¹⁴¹

Shi *et al.* have recently reported a new strategy for producing mesoporous silica-based rattle core-shell nanostructures, called the ‘controllable structural difference-based selective-etching strategy’.⁴ This method depends on the differences in the material structure rather than the composition, and consequently, due to large amounts of condensed Si–O–Si networks,

mesoporous silica shells will be less vulnerable to etching than the silica core, which is made of less condensed Si–OH bonds; this composition results in shell stability in the presence of sodium carbonate solution, while the cores dissolve to produce rattle structures. Implementing this method, Au-*meso*-SiO₂ and Fe₃O₄@*meso*-SiO₂ rattle core-shell nanoparticles have been obtained.⁴ Similarly, Zhao *et al.* have reported the selective etching of dense silica using alkaline solution while simultaneously maintaining mesoporous silica shell stability through condensation with the cationic surfactant, Cetyl trimethylammonium bromide molecules.^{146,147}

3.3.1.2. Surface-protected etching. This method was developed by Yin *et al.*^{119,148,149} and is based on a two step-process. The first step involves the adsorption of polyvinylpyrrolidone (PVP) polymer molecules onto the outer surface of silica spheres to stabilize this layer with hydrogen bonding between the polymer carbonyl groups and the hydroxyl groups of the silica surface. In the second step, a suitable etchant, such as NaBH₄ or NaOH, can be used to attack and dissolve the silica layer beneath the outer stabilized surface, which leads to the formation of rattle core-shell silica spheres.

3.3.2. Soft template assembly. The lack of control over size, morphology and composition of rattle structures prepared by the selective-etching process as well as the multiple tedious steps involved represent the main limitations of this approach. Soft templating methods have been effectively utilized to prepare rattle core-shell nanoparticles. (Max) Lu *et al.*⁸ have reported a general approach for constructing rattle structures using a fluorocarbon surfactant as a template. The resulting rattle-type spheres exhibited variable sizes, ranging from 200 to 700 nm, with different cores, including silica, gold, and Fe₃O₄ nanoparticles. In addition, Liu *et al.* have also shown that the shell thickness can be controlled and tuned to range from 10 to 50 nm.⁶² Soft templating methods have also been used to construct nanoreactors composed of Au rattle cores coated with ordered mesoporous organosilica (PMO) shells.¹⁵⁰ Similarly, magnetic rattle cores have been encapsulated by mesoporous PMO shells¹⁵¹ with the capability of tuning the rattle nanoparticle shell thickness and the magnetic character. The synthesized magnetic-PMO structures demonstrate many merits in addition to the magnetic character, including high surface area, large pore volume, and low density.

Another method of rattle core-shell nanoparticle fabrication is mixing two different types of surfactants, namely, sodium dodecyl benzenesulfonate (SDBS) and lauryl sulfonate betaine (LSB), as soft templates.¹⁵² Upon dispersion of nanoparticles into the surfactant mixture, rattle-type silica shells that have encapsulated the movable nanoparticles will be obtained.

3.3.3. The ship-in-bottle method. This method has been used previously to prepare loaded catalysts.¹⁵³ Using this method, large particle size cores can be formed within hollow particle structures^{154–156} through either chemical reaction or self-assembly. Qiao *et al.*¹⁵⁴ have fabricated multiple polymer dots encapsulated within hollow silica spheres through the ship-in-bottle method. Based on this approach, a single Au

nanoparticle was encapsulated within a porous polymer shell to construct a rattle structure.¹⁵⁴ In an alternative strategy, Ding *et al.* have utilized hydrated molten salts as metal oxide precursors that can diffuse more easily through mesoporous silica shells into the hollow cavities, fabricating the rattle nanostructure.¹⁵⁶ By conducting a calcination process, metal salts are converted to the corresponding metal oxides, resulting in a shell on the inner surface of the hollow silica spheres. Therefore, this reaction ends in double-shelled metal oxide-silica rattle nanostructures.

Shi *et al.*¹⁵⁷ have implemented this approach for fabricating Fe₂O₃@SiO₂ and Fe₃O₄@carbon rattle nanostructures (Fig. 11). By introduction of iron nitrate into the hollow mesoporous silica spheres followed by a calcination step, the iron nitrate will be converted to hematite nanocores, producing Fe₂O₃@SiO₂.

Fe₃O₄@carbon rattle nanostructures have been obtained by addition of furfuryl alcohol to the mesoporous silica shells with subsequent carbonization of the furfuryl alcohol to form carbon spheres. By the reduction of hematite cores, they will be converted to Fe₃O₄, and by dissolution of the remaining silica template, Fe₃O₄@carbon nanorattles will form.¹⁵⁷

3.3.4. The Ostwald ripening method. The Ostwald ripening is a physical method that involves re-crystallization of the materials in the solution phase (Fig. 12A).⁶² IUPAC has defined

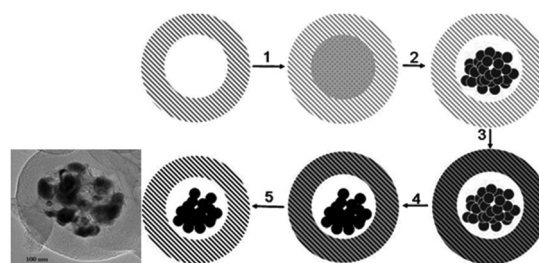


Fig. 11 Illustration of the synthesis procedure of hollow mesoporous carbon spheres with magnetic cores (HMCSMCs) by the ship-in-bottle approach: (1) introduction of the iron nitrate solution into the hollow core by vacuum nanocasting; (2) calcination into hematite particles of the core; (3) introduction of furfuryl alcohol into the mesoporous channels and polymerization; (4) carbonization of the polyfurfuryl alcohol, and the reduction of hematite particles into magnetic particles; and (5) removal of the silica template. (Reprinted with permission from John Wiley and Sons.)¹⁵⁷

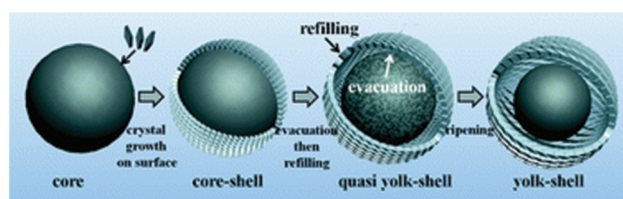


Fig. 12 Schematic procedure for the preparation of rattle core-shell nanoparticles by the Ostwald ripening approach. (Reprinted with permission from the Royal Society of Chemistry.)¹⁶²

the Ostwald ripening method as the “growth of larger crystals from those of smaller size which have a higher solubility than the larger ones”.¹⁵⁸ The Ostwald ripening method has received remarkable attention and has been widely used for preparation of many rattle-like nanomaterials.¹⁵⁹ Rattle core-shell metal oxide nanostructures including SnO₂, BaTiO₃, ZnO, Cu₃SO₄(OH)₄ and ZnS have been fabricated by the Ostwald ripening method.^{158–162} Cu₃SO₄(OH)₄ rattle core-shell nanostructures¹⁶¹ have been fabricated by Ostwald ripening, as shown in Fig. 12.¹⁶² The yolk-shell microspheres are formed from 2D nanoplates. The diameter of the yolk-shell spheres was controlled by adjusting the chelating agent concentration (1,3-propanediamine).¹⁶²

3.3.5. The galvanic replacement method. The galvanic replacement method can be considered a simple and facile tool for constructing metal nanoarchitectures having hollow cavities and porous shells.^{163–165} The governing step in this method is the replacement of a nanostructured metal template with another that is less active.⁶² Through galvanic replacement, a broad range of rattle Au nanoparticles having different shapes, such as nanoboxes, nanocages, and nanorings, have been successfully fabricated.⁶² Moreover, using this method, polyvinylpyrrolidone (PVP)-coated spherically clustered porous Au–Ag alloy nanorattles have been prepared by partial inhibition of galvanic replacement.¹⁶⁴

4. Applications for multifunctional nanomaterials

Applications of multifunctional core-shell nanomaterials can be versatile and cover many disciplines. The application suitability varies according to the core-shell, hollow core and rattle structure. The application suitability is also associated with the composition of the core and shell, as well as whether they are dense or porous. This section will shed light on the application versatility of each of these nanostructures.

4.1. Application of core-shell multifunctional nanomaterials

Core-shell particles have leading advantages over single particles in the biomedical and electronic fields. The following section will briefly discuss these applications.

4.1.1. Biomedical applications. In the field of biomedicine, useful and exciting applications of core-shell nanoparticles have been developed over the past decade. However, in areas of major importance, some main applications are still in their innovative phase.^{166,167} The key applications of core-shell nanoparticles include drug delivery,^{168–171} bioimaging techniques^{168,169,171} and biosensors.^{172–174}

4.1.1.1. Drug delivery and specific targeting. Recent studies have shown a tremendous improvement in the performance of drug delivery systems due to the development of controlled drug release, which is much superior to conventionally uncontrolled release. With the advent of nanotechnology, the progress made in these areas has swiftly become faster and more precise. Moreover, “targeted delivery” is the process in which a

particular location inside a body or organ can be intentionally and precisely targeted using a very specific drug delivery system. Therefore, a controlled drug delivery system combined with specific targeting capability is a very potent technology to be explored and exploited. For more improvement of the drug delivery system, the essential properties of free drugs, such as solubility, *in vivo* stability, pharmacokinetics, and bio-distribution, need to be comprehensively studied. The overall effectiveness of a controlled delivery system with specific targeting ability can be significantly enhanced using well-designed drug carrier nanoparticles that can selectively target particular tissues.¹⁷³

In designing these exceptional nanoparticles for targeted drug delivery, the process first involves the encapsulation of the drug inside the mesoporous nanoparticles with suitable surface coatings for the selective attachment to a specific cell surface. Second, upon reaching the target cell site, these nanocarriers will disintegrate or open up supramolecular gates that are chemically attached to the outlet of the mesopores and release their drug cargo.

The release of the drug cargo from the coated nanoparticle carriers will be triggered either by an external stimulus such as heat or light or by a stimulus of the target cell chemical environment, such as pH or specific ion concentration. By further coating the carrier with fluorescent active material, these core-shell nanoparticles, which can be considered as sensors, can also be tracked to confirm the delivery of the drug to a specific site. Consequently, iron oxides, Fe, Ni, Co, and super paramagnetic iron oxide nanoparticles are often used as core particles to design and produce magnetic nanoparticles with suitable shell coatings for *in vivo* drug release and sensor applications.^{175–179} Currently, magnetic-polymer core-shell nanoparticles are typically utilized for drug delivery, cell labeling and separation,^{180,181} and tumor delineation.¹⁸² Further, owing to their biocompatibility with living cells, magnetic@polymer and magnetic@SiO₂ nanoparticles offer more advantages over bare magnetic nanoparticles and are therefore more explored for drug delivery studies.^{177,179}

4.1.1.2. Bioimaging. There are different types of molecular bioimaging techniques used for both *in vivo* and *in vitro* biological specimens. These include optical imaging (OI), magnetic resonance imaging (MRI), and ultrasound imaging. Among these, optical and magnetic resonance techniques have used the inherent luminescent and magnetic nanoparticle properties and are therefore the most suitable among all other techniques. The luminescent nanoprobe used for optical imaging and the magnetic nanoparticles used for magnetic resonance imaging are the two main types of nanoparticles widely used for *in vivo* imaging. The dual-mode of simultaneous optical and magnetic resonance imaging can be accomplished with core-shell nanostructures.^{182–184} These nanoprobe used for optical imaging normally utilize quantum dots (QDs) or dye-doped QDs. However, the main concerns of QDs are their high level of toxicity as well as their ease of photo-oxidation. These disadvantages can be minimized by coating them with appropriate materials to form a

core-shell structure that can be straightforwardly utilized for *in vivo* optical imaging.^{185,186}

Another technique that can be explored for tumor cell imaging is the surface plasmon effect of Ag metal, such that a smart-gel polymer-coated Ag nanoparticle can serve as an effective local delivery system to a tumor site.¹⁸⁷ Fig. 13 shows a Ag@hydrogel core-shell structure imaging technique where a Ag nanoparticle, the delivery system, was accomplished using a pH-sensitive hydrogel to release drugs under different pH conditions. The detection of tumor cells can be made possible by the deposition of core-shell nanoparticles onto tumor cells followed by light exposure up to 500 ms to induce fluorescence emission. Fluorescence and photoluminescence properties can also be used for cell imaging with materials from the lanthanide earth metal group. Lanthanide metal salts have good luminescence properties, and with well-designed biocompatible shell coatings, these materials can be utilized for the imaging and biodetection of cells in living systems. With appropriate doping of lanthanide ions such as Er, Tm, or Yb onto nanoparticles, emission spectra can be shifted to green, red, or blue wavelengths with increased intensity.^{188–190}

4.1.1.3. Sensors. Sensors are input devices that assess and quantify a physical property and convert it into an analog/digital signal, which can then be interpreted by another instrument. In the detection of DNA, RNA, glucose, and cholesterol, among others, nanoparticles are often used as sensors for *in vivo* applications. In this regard, magnetic@fluorescence nanoparticles can be utilized as sensors, where the fluorescent dye tracks the location of the particle, and the magnetic shell conducts heat *via* magnetic excitation.¹⁷⁵ These magnetic nanocomposites can be further coated with many other materials, such as metals, silicas, or polymers, that represent bioanalytical sensors.^{191–193}

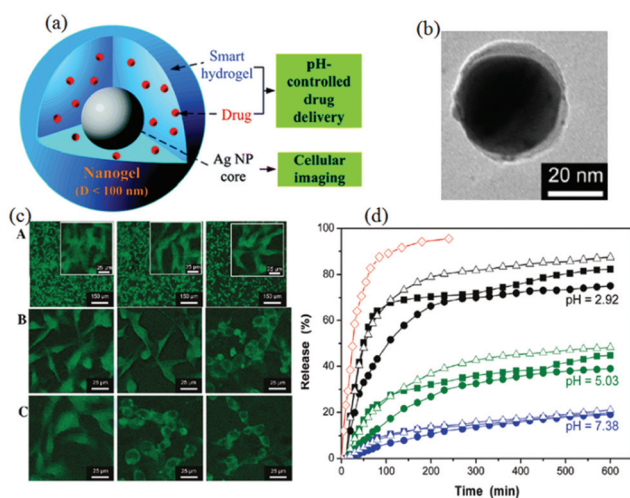


Fig. 13 (a) Schematic illustration for integration of tumor cell imaging and pH-triggered drug delivery. (b) TEM image of drug-loaded core-shell hybrid nanogels with the smart-gel shell coated on the Ag nanoparticle core. (c) Scanning confocal images of B16F10 cells incubated with hybrid nanogels. (d) Drug release profiles at different pH levels. (Reprinted with permission from the American Chemical Society.)¹⁸⁷

Similarly, ZnS/Mn@SiO₂ nanoparticles have been implemented as sensors for Cu²⁺ ions.¹⁹⁴ Other sensor materials such as the bimetallic core-shell nanoparticles can also be used for *in vivo* applications. Cancer and tumor cells in the body can both be sensed using Au/Ag core-shell composite nanoparticles.¹⁹⁵ However, functionalization of these particles with antibodies for selective binding with analyte molecules has remained an issue and thus limits their potential applications. Magnetic core-shell-based sensors such as Fe/Fe₂O₃ core-shell nanoparticles are also selectively utilized for the detection of damaged DNA,¹⁹⁶ where bioactive proteins, such as cytochrome P450, myoglobin (Mb) and hemoglobin (Hb), are attached to the magnetic particles to mimic *in vivo* toxicity.¹⁹⁷

4.1.2. Catalytic applications. The physical properties (*e.g.*, optical, catalytic, electrical, and magnetic) of magnetic materials can be greatly enhanced by coating them with functional materials such as noble metals, semiconductors, or appropriate oxides, especially compared with those of uncoated magnetic materials.^{198–200} For example, upon coating a transition metal oxide, such as Fe₂O₃²⁰¹ and V₂O₅,²⁰² onto nanosized metal oxides (MgO, CaO), the destructive absorption capacity of the latter toward halogenated hydrocarbons and organophosphorus has increased several-fold. Ding *et al.* have fabricated separable catalyst Fe₃O₄@SiO₂-Au@m-SiO₂ core-double shell particles as highly integrated catalysts for the catalytic reduction of 4-nitrophenol and styrene epoxidation (Fig. 14).²⁵ The catalytic epoxidation of styrene using the multifunctional microspheres showed high conversion and good selectivity without being washed away and disengaged from the support, as in the case of separate gold nanoparticles. In this regard, the core-shell-integrated nanocatalyst was designed to avoid the washing issue.

Yin *et al.*¹⁹⁹ reported that the efficiency of the catalytic conversion of CO to CO₂ by Fe₂O₃-coated Au nanoparticles supported on SiO₂ increased considerably compared with the uncoated Au supported on SiO₂.

Furthermore, it has also been reported that, although catalyst pre-heating increases its efficiency, excess heating can also decrease efficiency due to an increase in the percentage of Au

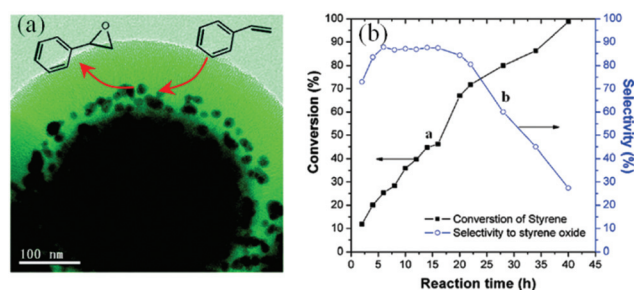


Fig. 14 (a) TEM image and (b) the conversion of styrene and selectivity of styrene oxide over multifunctional Fe₃O₄@SiO₂-Au@m-SiO₂ core-double shell nanoparticles as a highly integrated catalyst system. (Reprinted with permission from the American Chemical Society.)²⁵

metals and crystallinity of the Fe_2O_3 shell. Similarly, the stability of metal cores (such as Fe, Co, Ni) coated with porous silica shells was also markedly increased, together with enhanced catalytic activity for the production of Cox-free H_2 during NH_3 decomposition.²⁰³ Bimetallic core-shell nanoparticles have shown higher catalytic activity upon comparison with single uncoated metal nanoparticles, which can be attributed to a synergistic effect. Furthermore, catalysts such as bimetallic core-shell nanoparticles,²⁰⁴ such as Au/Pd^{205–207} and Au/Ag,^{208,209} have been widely used in a range of catalytic reactions.

4.2. Application of hollow core-shell multifunctional nanomaterials

Hollow-based structures exhibit low density, low refractive indices and low thermal expansion coefficients. These characteristics make them highly important for many applications in different fields, including energy storage, antireflection coatings and catalyst support. The synthesis and modification of hollow structures continue to improve their mechanical, electrical and chemical properties to make them more suitable for drug delivery, therapeutics, fluorescence, and lithium-ion batteries. In this section, applications of hollow core-shell nanostructures in energy storage, catalysis and biomedicine will be presented.

4.2.1. Lithium-ion batteries. Lithium-ion batteries are the most frequently used power source for electronic devices as well as for electric automobiles due to their low self-discharge rates. In addition, lithium-ion batteries are known to have a high energy density.²¹⁰ However, current electrode materials may limit their performance due to the low efficiency in charge-discharge rates.²¹¹ For example, graphitic carbon is the most used anode electrode, but due to their limited gravimetric capacity, researchers have begun to seek other electrodes with higher capacities at low potentials. For this purpose, many materials have been tested to implement a new strategy instead of the classical Li insertion/deinsertion. The new strategy depends on two reaction processes; the first is Li-metal alloying/de-alloying for metals (Si, Sn/ SnO_2 , Al, Sb),^{212–214} the second is the reversible formation-decomposition of Li_2O nanomaterials for transition metal oxides such as CoO, NiO and FeO .²¹⁴ The aim of this development is to enhance the cycling life, energy density and charge-discharge rate.

Shen *et al.* have synthesized uniform NiCo_2O_4 hollow spheres with complex interior structures for lithium-ion batteries and super-capacitors.¹³² NiCo_2O_4 hollow spheres exhibited a core double-shell interior architecture, and the porous shells were formed from tiny nanoparticles. Upon being tested as electrode materials for both lithium-ion batteries and super-capacitors, NiCo_2O_4 hollow spheres manifested superior electrochemical performance. Additionally, Mo-doped SnO_2 mesoporous hollow-structured spheres were synthesized and utilized as anode materials for high-performance lithium-ion batteries.²¹⁵ Mo-doped SnO_2 lithium-ion battery anodes have showed enhanced electrochemical performance with good cycling stability, high specific capacity and high rate capability.

Hollow Mo-doped SnO_2 nanoparticles showed a specific capacity of 801 mA h g^{-1} for 60 cycles at a current density of 100 mA g^{-1} , which represents a 1.66-fold improvement over the pure SnO_2 hollow nanoparticles. Moreover, even if the current density reached 1600 mA g^{-1} , it still preserves its stability at a specific capacity of 530 mA h g^{-1} , which suggests that it has an extraordinary rate capability.

Wu *et al.*²¹⁶ have also fabricated hollow spherical $\text{Li}_{1.2}\text{Mn}_{0.54}\text{Ni}_{0.13}\text{Co}_{0.13}\text{O}_2$ cathodes by homogeneous precipitation-hydrothermal synthesis. As a lithium-ion battery cathode, it possessed an initial discharge capacity of $286.4 \text{ mA h g}^{-1}$ at 0.1 C between 2.0 and 4.8 V and a discharge capacity of $240.9 \text{ mA h g}^{-1}$ that could be retained after 50 cycles. The hollow spheres were assembled into plate-like nanoparticles, which helped improve the rate performance due to fast transmission of Li^+ from the cathode to electrolyte.

4.2.2. Catalysis and photocatalysis. The developments of the hollow core-shell nanomaterials have led to significant growth of their use in the catalysis field. For example, Kim *et al.*²¹⁷ have used hollow palladium nanospheres as efficient catalysts for Suzuki coupling reactions, which led to an improvement of the catalytic activity even after seven times reuse and the reduction of Pd leaching. In addition, bimetallic hollow PdCo nanospheres have been utilized to improve the yield of Sonogashira reaction catalysis in aqueous media.²¹⁸ Another example is the usage of the hollow structures of $\text{Ni}_{1-x}\text{Pt}_x$ to enhance NH_3BH_3 reactions to release H_2 due to the hollow spheres' superior catalytic activities, which can be related to the high surface area (Fig. 15).²¹⁹ Compared to dense spheres of the same size, the hollow structure is more effective as a catalyst because it allows the outer and inner surfaces to interact with the reactants. Zhou *et al.*²²⁰ have synthesized Pd@ TiO_2 hollow core-shell nanospheres as an efficient and reusable catalyst for the reduction of *p*-nitrophenol with NaBH_4 aqueous solution at room temperature. In addition, this material showed a high recyclability through extensive reuse (eight times) without a pronounced loss of activity.

Porous ceria (CeO_2) hollow nanospheres decorated with Au nanoparticles have been synthesized by a simple one-step solvothermal reaction. Au/ CeO_2 hollow core spheres were used as

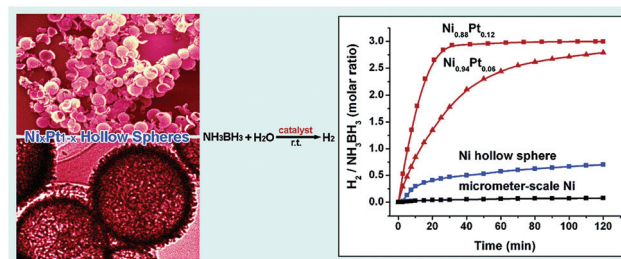


Fig. 15 Impact of alloy and hollow structure on hydrogen gas production through NH_3BH_3 reaction. (Reprinted with permission from the American Chemical Society).²¹⁹

the catalyst for CO oxidation. These results showed that the CO conversion by hollow spheres reached 92% at ambient temperature. Moreover, the CO conversion was maintained at 91% after the catalyst had been continuously used for 20 h.²²¹

Hollow hierarchical Ni/ γ -Al₂O₃ nanocomposites have been prepared by the hydrothermal method for methane dry reforming catalysis. Due to their hollow structure, Ni/ γ -Al₂O₃ nanocomposites have shown coke and sintering resistance in long-term dry reforming of methane at 750 °C.²²² Furthermore, the hollow structures have shown remarkable performance as catalysts for electrocatalytic and photocatalytic applications. An advantage of the reported hollow nanostructures is that they can be made with metal/metal oxide particles that are suitable for oxidation of methanol, ethanol and formic acid. The introduction of hollow core-shell Pt structures has resulted in doubling its catalytic activity compared with similarly sized solid Pt nanoparticles.²²³ In addition, constructing noble metal hollow structures enables significant improvement of their electrocatalytic activities,^{49,224} which could be attributed to their high electrochemical surface area, in addition to the hollow structure that provides enough space to accommodate large numbers of loaded molecules.⁹

Wang *et al.* have recently developed hollow graphitic carbon nitride nanosphere photocatalysts with enhanced photocatalytic activity.^{225–230} They have successfully synthesized hollow g-C₃N₄ nanospheres by a hard templating method using silica nanoparticles, where the deformation of hollow g-C₃N₄ nanospheres was prevented by controlling the shell thickness of the hollow spheres.²²⁵ Furthermore, they have enhanced the surface, crystal and textural structures of the hollow g-C₃N₄ nanospheres by optimizing the post-annealing process.²²⁷ The photocatalytic hydrogen evolution of the hollow g-C₃N₄ nanospheres was boosted by shell engineering,²²⁸ doping with CdS quantum dots²²⁹ as well as integration with Au and CdS, nanoparticles and quantum dots, respectively.²³⁰

4.2.3. Biomedical applications. Many nanoparticles have been reported to be used in various biomedical applications, such as drug delivery and bio-imaging.^{231–233} However, the nanoparticles based on hollow structures are superior for gene delivery, imaging, therapeutic uses and other biomedical applications. Silica represents the most commonly used hollow structure for such purposes due to its non-toxic nature. In addition, hollow silica spheres showed high biocompatibility and facile bio-conjugation through silane chemistry.^{234–236} Furthermore, the hollow silica spheres have been utilized as drug nanocarriers because the drugs can be released from their hollow structures in a controlled fashion.^{234,235,237} An extra advantage of hollow silica spheres is the possibility of having additional special properties through surface functionalization. In this regard, Zhu *et al.* have coated hollow silica spheres with polyelectrolyte multi-layers for constructing stimuli-responsive drug release systems that can be controlled by adjusting the pH values. In this regard, such systems possess the advantages of high drug storage capacity as well as stimuli-responsive behavior (Fig. 16).

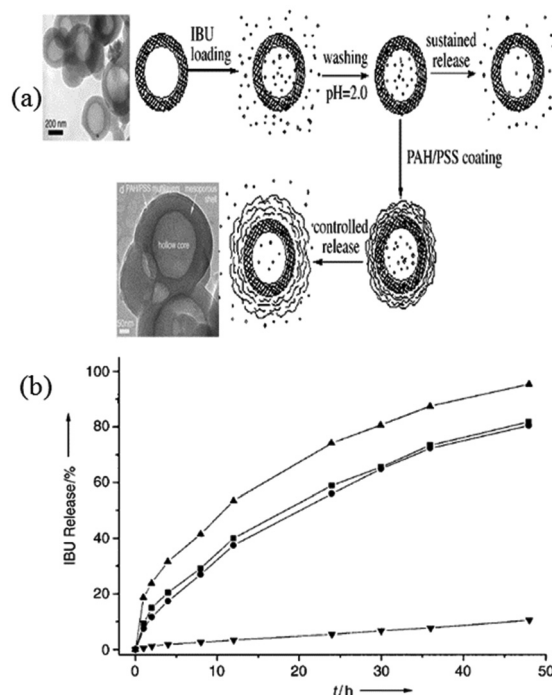


Fig. 16 (a) Schematic illustration of two drug delivery systems that give different controlled release patterns and (b) cumulative drug release of the two systems in media of different pH values. ■: pH 1.4 from IBU-HMS, ●: pH 1.4 from IBU-HMS@PEM, ▲: pH 8.0 from IBU-HMS, ▼: pH 8.0 from IBU-HMS@PEM. (Reprinted with permission from John Wiley and Sons.)⁵

Delivering genetic material to cells is another function that can be achieved by hollow nanostructures. For example, preparation of calcium phosphate multi-shell hollow nanostructures for encapsulating DNA has been reported by Sokolova *et al.*²³⁸ These hollow core nanostructures showed better transfection efficiency than the normal DNA-coated calcium phosphate nanoparticles. This may be attributed to the presence of multi-layers that enable the sequential delivery of various agents with more flexibility. Recently, Cai *et al.* have reported the application of hollow calcium phosphate spheres as drug carriers.²³⁹ The loading of the drug molecules onto the hollow core spheres was achieved by encapsulation during synthesis, while the drug release trigger was accomplished using ultrasonic waves.

The hollow gold nanostructures showed excellent optical properties suitable for imaging and diagnostic applications. For example, hollow gold nanocages with porous walls have been used as an optical coherence tomography contrast agent, as reported by Chen *et al.*²⁴⁰ Additionally, the galvanic replacement reaction between silver templates and chloroauric acid has been used for the preparation of hollow gold nanocages.²⁴¹ The tuning of the gold nanocage size is reported to make them strongly absorb in the near infra-red region (NIR), which has optimal optical transmission through tissue. A therapeutic effect (*i.e.*, photothermal therapy) on targeted cancer cells has

been achieved by targeting cancer cells with gold nanocages and irradiating them with infrared light, which led to local, irreversible ablation that killed the cancer cells.^{241,242} This new technique is considered to be an effective platform for cancer treatment and is more promising than chemotherapy or surgery approaches.

4.3. Application of rattle core-shell multifunctional nanomaterials

The wide spectrum of unique and interesting properties that rattle core-shell nanostructures possess, *e.g.*, low density, movable core with void space between the core and the shell, and the ready tailor-ability and functionality of both cores and shells, provide for remarkable and diverse applications. In the following section, nanorattle applications such as nanoreactors, photocatalysts, and drug delivery agents will be reviewed.

4.3.1. Catalysis. Nanoreactors²⁴³ can be defined as ultra-small reaction containers that contain a catalyst inside their boundaries. Their advantages stem from their ability to hold reagents and catalysts for a long period of time and their ability to protect catalysts from environmental influences; these features greatly improve chemical transformation processes. In general, nanoreactors are required to have three main characteristics: provide for rapid diffusion of reactants and products; provide protection for the nanocatalysts; and have long-term stability.⁶² Rattle core-shell nanostructures exhibit all these characteristics. Rattle shells provide the protection of the catalytic nanocores while simultaneously enabling the rapid diffusion of the reactants and products. The rattle nanocore, as an active catalyst, boosts catalytic activity, while the cavity between the core and the shell creates a homogeneous environment for the reaction to take place.⁶²

Rattle gold nanoreactors have been utilized to reduce *p*-nitrophenol, 2-nitroaniline, benzimidazole derivative oxidation of aerobic alcohol, and CO oxidation.^{68,72,74,244–248} Au-SiO₂ yolk-shell nanoreactors have shown promising catalytic activity for CO oxidation with high stability after long-term recyclability and storage. The CO oxidation reaction was successfully controlled by the corking design using the capillary condensation of water vapor for corking the mesopores within the shell. However, at higher temperatures or lower water vapor pressures, water evaporates, which opens the mesopores and causes the water to promote the CO oxidation reaction. In this regard, both the corking and uncorking mechanism of the Au-SiO₂ yolk-shell nanoreactor is reversible (Fig. 17).²⁴⁸

Rattle type multi-core Au@poly(styrene-*co*-methylacrylic acid) (PS-*co*-PMAA) nanoreactors can be utilized to synthesize acids *via* aerobic alcohol oxidation.²⁴⁶ Inside the nanoreactors, the reaction will proceed more efficiently and will provide quantitative yield after 30–120 min. Moreover, the turnover frequency (TOF) will be approximately 100 to 400 h⁻¹.²⁴⁶

Encapsulation of other metal or metal oxide nanoparticles into the hollow spheres to form rattle core-shell nanoreactors, such as Ni,²⁴⁹ Cu,²⁵⁰ Pt,¹⁰⁶ Pd,²⁵¹ and Ag,^{252,253} has also been reported. Li *et al.* synthesized yolk-satellite-shell structured Ni-yolk@Ni@SiO₂ nanoparticles for the CO₂ (dry) reforming

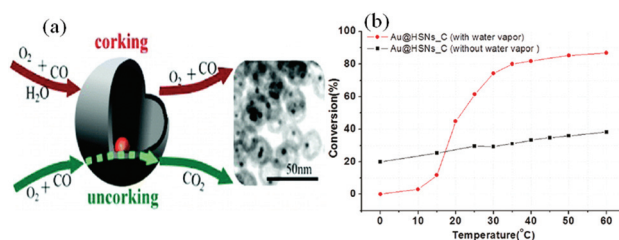


Fig. 17 (a) Scheme of corking and uncorking a catalytic activity of an Au-SiO₂ yolk-shell nanoreactor and (b) CO conversion of Au@HSNs_C with GHSV = 360 000 mL g_{cat}⁻¹ h⁻¹ (1%CO/6%O₂/93%He) under vapor and vapor-free conditions in a temperature range of 0–60 °C. (Reprinted with permission from the American Chemical Society.)²⁴⁸

of methane at different shell thicknesses.²⁴⁹ At a 11.2 nm shell thickness, Ni-yolk@Ni@SiO₂ showed near equilibrium conversion for CH₄ and CO₂ for 90 h at 800 °C, together with very negligible carbon deposition.²⁴⁹

Rattle Pd@mesoporous silica nanoreactors have shown high activity rates for the Suzuki cross-coupling reactions, with reaction completion after 3 min.²⁵¹ Moreover, Pd leaching was substantially minimized, which confirms stable catalytic performance. In addition, the RGO@Pd@C nanohybrid exhibits superior and stable catalytic performance by converting 4-nitrophenol (4-NP) to 4-aminophenol within only 30 seconds.²⁵⁴

4.3.2. Photocatalysis. Rattle core-shell nanostructures can provide remarkable enhancement to photocatalytic activity.^{255–258} Rattle core-shell titania microspheres have been fabricated using the solvothermal method through mixing glycerol, alcohol, ethyl ether and TiO₅O₄.²⁵⁶ A phenol degradation test showed 93% conversion due to the rattle core-shell structures. A suitable selection of the core size is believed to permit multiple UV light reflections within the interior cavity, which enhances light usage efficiency and hence improves the photocatalytic activity. Furthermore, on constructing Au@r-GO/TiO₂ yolk@shell nanostructures, the evaluation of visible light showed photocatalytic activities in dye decomposition and water-splitting H₂ production (Fig. 18).²⁵⁷ In addition, an enhanced photocatalytic activity was obtained using small Fe₃O₄@TiO₂ with a unique yolk-shell structure below 50 nm.²⁵⁸

4.3.3. Biomedical applications. Due to their tailorable void space, controllable size, and good biocompatibility, the rattle core-shell nanostructures are considered as promising drug delivery nanocarriers. Because of their cavities, rattle core-shell nanostructures have a high loading capacity as well as efficient delivery of drug, protein and nucleic acid molecules. In addition, to obtain a variety of desired properties, nanorattle interiors can be functionalized by encapsulating materials that exhibit the desired functionalities, such as fluorescent molecules and QDs.^{77,259–263} In this section, some of the biomedical applications for magnetic nanorattle core-shell nanostructures will be addressed.

Du *et al.* have fabricated polymer-based nanorattle spheres with combined thermo- and pH-responsive capabilities for

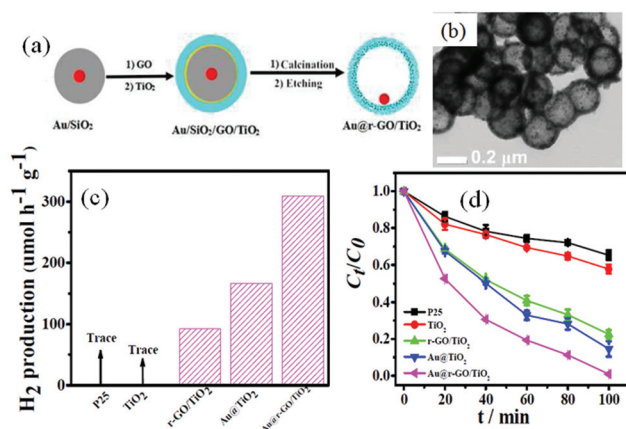


Fig. 18 (a) Schematic procedure for the preparation of Au@r-GO/TiO₂ yolk-shell nanostructures, (b) TEM image of Au@r-GO/TiO₂, and the evaluation of visible light photocatalytic activity for (c) RhB dye decomposition and (d) water-splitting H₂ production. (Reprinted with permission from the American Chemical Society.)²⁵⁷

controlling the release of cancer treatment drugs. Both the yolk and the shell have shown different functions; while pH-induced thermally responsive polymer shells serve as smart “valves” that control the diffusion of the drugs in/out of the polymer nanorattles based on the surrounding environments, the P(MAA-co-EGDMA) yolk improves the loading capacity of cancer drugs such as doxorubicin hydrochloride (DOX).²⁶²

In another study, radioluminescent yolk-upconverting shell nanoparticles have been obtained by encapsulation of the radioluminescent nanophosphor core nanoparticles within silica shells. Furthermore, by partial etching of nanophosphors in acid media and coating silica shells with a second upconverting shell, yolk-shell structures have been produced. The nanoparticles showed multiple functionalities, such as pH-triggered drug release and radioluminescence, upconversion luminescence, and combined magnetic resonance (MRI) imaging.²⁶³

It is known that iron oxide nanoparticles have great potential for nano-biomedical applications, such as magnetic contrast agents, magnetic drug targeting, and hyperthermic tumor treatments.¹¹ Rattle core-shell nanostructures became desirable for their ability to improve the stability and biocompatibility of iron oxides in biomedical applications.^{260–262} Rattle Fe₃O₄@NiSiO₃ nanostructures have been implemented with a high specificity for histidine protein purification from the mixtures of lysed cells. Fe₃O₄@NiSiO₃ nanorattles have shown high recyclability, where Ni²⁺ cations within the shell provided docking sites for selective coordination with histidine.²⁶⁰ Furthermore, yolk-shell gold-metal oxide nanoparticles have been used for targeting and eliminating cancer cells by photothermal/chemotherapy strategies.^{77,78} Zhang *et al.*⁷⁷ have proposed yolk-shell gold nanorod@void@mesoporous titania nanoparticles (AuNR@void@m-TiO₂ NPs) for combined chemo-photothermal therapy and SERS imaging. The Raman reporters were loaded on AuNRs, and then the doxorubicin (DOX) cancer drug was loaded into the m-TiO₂ rattle structure

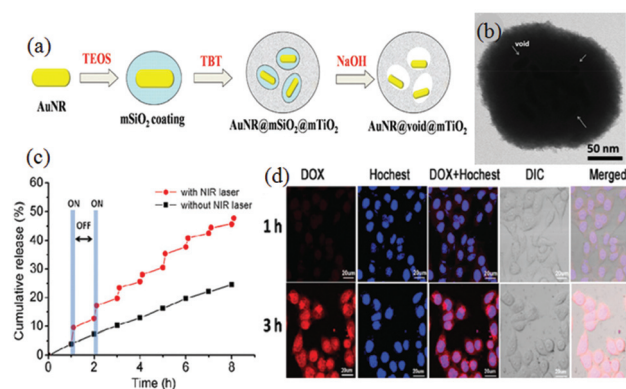


Fig. 19 (a) Schematic illustration and (b) HR-TEM image of yolk-shell gold nanorod@void@mesoporous titania nanoparticles (AuNR@void@m-TiO₂ NPs). (c) DOX release profiles from DOX-loaded NPs with and without 785 nm NIR laser in PBS buffer (pH 5.0). (d) Confocal laser scanning microscopy images of MCF-7 cells taken after treatment with DOX-loaded NPs at different incubation times. Hoechst 33342 was used for cell nuclei staining (blue fluorescence). Red fluorescence in the MCF-7 cells originated from DOX. (Reprinted with permission from the Royal Society of Chemistry.)⁷⁷

(Fig. 19). The obtained SERS signal was strong and was detected easily in both living cells and mice. The m-TiO₂ showed promising drug loading and release performance compared with m-SiO₂, yet it was more chemically inert, which provided it with increased structural stability in biological systems. Furthermore, the near infrared (NIR) light absorbing character of the Au nanoparticle yolk was also tested for drug-release regulation and photothermal treatment; this test resulted in superior elimination of MCF-7 cells upon combined treatment with DOX-encapsulated nanoparticles and NIR laser illumination, which can be associated with a synergistic chemo-thermal therapeutic effect.⁷⁷

Veres *et al.*²⁶⁴ have fabricated fluorescent Fe₃O₄@SiO₂ nanorattles with Fe₃O₄/Au dumbbell-like nanocores and mesoporous silica shells that are rich in primary and secondary amine groups, which are important for coupling biomolecules. The fabricated nanorattles have shown various magnetic, plasmonic, and fluorescence properties as well as the ability to accommodate biomolecules.

5. Conclusions and outlook

Nanotechnology has entered a new research era with the primary research goal of constructing a novel class of substances, known as multifunctional nanomaterials, to achieve outstanding performances and accomplish novel applications. Surface-coating techniques have opened ways to achieve nanomaterial multifunctionality by constructing newly designed core-shell nanostructures. Studies have evolved and different design strategies and fabrication approaches to engineer different types of core-shell nanoparticles in diverse core and shell combinations, with materials including metals, metal

oxides, and polymers have been continually pursued. The manipulation of shell characteristics (*e.g.*, density) as well as the growth of multiple shells have provided tremendous opportunities for an unlimited number of functionalities. The need for multifunctional nanoparticles with specialized functions, such as superior storage capacity, has also been met through the core removal of core-shell nanostructures. Synthesis approaches, such as hard and soft templating, have been used to construct hollow core-shell nanostructures. Special designs for multiple-shell hollow core nanoparticles with versatile and diverse functions have also been investigated. Furthermore, material scientists have continuously pursued designs for tailoring new architectures based on the core-shell system, which has resulted in rattle core-shell nanoparticles. This newly developed architecture merges the properties and geometries of the solid core systems with those of the hollow systems to provide new structures described as having a core@void@shell configuration. This rattle-type structure possesses characteristics and functions of both systems in a single particle. The number of research papers published annually in the field of multifunctional core-shell, hollow core, and rattle core-shell nanoparticles has increased significantly. The applications of such nanomaterials are being explored in new fields of nanotechnology, while at the same time merging other nanotechnology disciplines. However, one of the many challenging aspects of this novel class of materials is the flexibility of the fabrication approach for the production of homogeneous and uniform nanoparticles. Additionally, scaling-up is the most important issue to be resolved for the future production of multifunctional nanoparticles in commercial-scale quantities.

Acknowledgements

This work was supported through the project funded by the National Plan for Science, Technology and Innovation (MAARI-FAH), King Abdulaziz City for Science and Technology, Kingdom of Saudi Arabia, Award Number (12-NAN2544-02).

References

- 1 W. Zhao, J. Gu, L. Zhang, H. Chen and J. Shi, *J. Am. Chem. Soc.*, 2005, **127**, 8916.
- 2 J. Kim, H. S. Kim, N. Lee, T. Kim, H. Kim, T. Yu, I. C. Song, W. K. Moon and T. Hyeon, *Angew. Chem., Int. Ed.*, 2008, **47**, 8438.
- 3 J. Hu, M. Chen, X. Fang and L. Wu, *Chem. Soc. Rev.*, 2011, **40**, 5472.
- 4 Y. Li and J. Shi, *Adv. Mater.*, 2014, **26**, 3176.
- 5 Y. Zhu, J. Shi, W. Shen, X. Dong, J. Feng, M. Ruan and Y. Li, *Angew. Chem., Int. Ed.*, 2005, **44**, 5083.
- 6 J. Yuan, K. Laubernds, Q. Zhang and S. L. Suib, *J. Am. Chem. Soc.*, 2003, **125**, 4966.
- 7 A. M. El-Toni, M. A. Habila, M. A. Ibrahim, J. P. Labis and Z. A. Al Othman, *Chem. Eng. J.*, 2014, **251**, 441.
- 8 J. Liu, S. Z. Qiao, S. B. Hartono and G. Q. M. Lu, *Angew. Chem., Int. Ed.*, 2010, **49**, 4981.
- 9 X. W. Lou, L. A. Archer and Z. Yang, *Adv. Mater.*, 2008, **20**, 3987.
- 10 Y. Zhao and L. Jiang, *Adv. Mater.*, 2009, **21**, 3621.
- 11 J. Liu, S. Z. Qiao, Q. H. Hu and G. Q. M. Lu, *Small*, 2011, **7**, 425.
- 12 J. C. Park and H. Song, *Nano Res.*, 2011, **4**, 33.
- 13 Q. Zhang, W. S. Wang, J. Goebel and Y. D. Yin, *Nano Today*, 2009, **4**, 494.
- 14 A. M. Cao, R. W. Lu and G. Vesper, *Phys. Chem. Chem. Phys.*, 2010, **12**, 13499.
- 15 A. Henglein, *Chem. Rev.*, 1989, **89**, 1861.
- 16 L. Spanhel, H. Weller and A. Henglein, *J. Am. Chem. Soc.*, 1987, **109**, 6632.
- 17 H.-C. Youn, S. Baral and J. H. Fendler, *J. Phys. Chem.*, 1988, **92**, 6320.
- 18 C. F. Hoener, K. A. Allan, A. J. Bard, A. Campion, M. A. Fox, T. E. Malluok, S. E. Webber and J. M. White, *J. Phys. Chem.*, 1992, **96**, 3812.
- 19 I. Honma, T. Sano and H. Komiyama, *J. Phys. Chem.*, 1993, **97**, 6692.
- 20 H. S. Zhou, H. Sasahara, I. Honma, H. Komiyama and J. W. Haus, *Chem. Mater.*, 1994, **6**, 1534.
- 21 R. G. Chaudhuri and S. Paria, *Chem. Rev.*, 2012, **112**, 2373.
- 22 Y. K. Jun, J. Choi and J. W. Cheon, *Chem. Commun.*, 2007, 1203.
- 23 C. M. Niemeyer, *Angew. Chem., Int. Ed.*, 2001, **40**, 4128.
- 24 X. F. Zhang, S. Mansouri, L. Clime, H. Q. Ly, L. 'H. Yahia and T. Veres, *J. Mater. Chem.*, 2012, **22**, 14450.
- 25 Y. Deng, Y. Cai, Z. Sun, J. Liu, C. Liu, J. Wei, W. Li, C. Liu, Y. Wang and D. Zhao, *J. Am. Chem. Soc.*, 2010, **132**, 8466.
- 26 S. H. Joo, J. Y. Park, C.- Tsung, Y. Yamada, P. Yang and G. A. Somorjai, *Nat. Mater.*, 2009, **8**, 126.
- 27 M. Ma, H. Chen, Y. Chen, X. Wang, F. Chen, X. Cui and J. Shi, *Biomaterials*, 2012, **33**, 989.
- 28 C. Barbé, J. Bartlett, L. Kong, K. Finnie, H. Q. Lin, M. Larkin, S. Calleja, A. Bush and G. Calleja, *Adv. Mater.*, 2004, **16**, 1959.
- 29 H. M. Beigi, S. Yaghmaei, R. Roostaazad and A. Arpanaei, *Physica E*, 2013, **49**, 30.
- 30 Y. Deng, Y. Cai, Z. Sun and D. Zhao, *Chem. Phys. Lett.*, 2011, **510**, 1.
- 31 V. V. Srdić, B. Mojić, M. Nikolić and S. Ognjanović, *Process. Appl. Ceram.*, 2013, **7**, 45.
- 32 F. Caruso, *Adv. Mater.*, 2001, **13**, 11.
- 33 S. Karele, S. W. Gosavi, J. Urban and S. K. Kularni, *Curr. Sci.*, 2006, **91**, 1038.
- 34 Y. Piao, A. Burns, J. Kim, U. Wiesner and T. Hyeon, *Adv. Funct. Mater.*, 2008, **18**, 3745.
- 35 A. Guerrero-Martinez, J. Perez-Juste and L. M. Liz-Marzan, *Adv. Mater.*, 2010, **22**, 1182.
- 36 R. Hao, R. Xing, Z. Xu, Y. Hou, S. Gao and S. Sun, *Adv. Mater.*, 2010, **22**, 2729.
- 37 Y. Zhu, Y. Fang and S. Kaskel, *J. Phys. Chem. C*, 2010, **114**, 16382.

- 38 J. Liu, F. Liu, J. Wu and D. Xue, *J. Mater. Chem.*, 2009, **19**, 6073.
- 39 H. P. Liang, L. J. Wan, C. L. Bai and L. Jiang, *J. Phys. Chem. B*, 2005, **109**, 7795.
- 40 J. Chen, D. Wang, J. Qi, G. Li, F. Zheng, S. Li, H. Zhao and Z. Tang, *Small*, 2015, **11**, 420.
- 41 J. W. Leem, S. Kim, C. Park, E. Kim and J. S. Yu, *ACS Appl. Mater. Interfaces*, 2009, **1**, 1070.
- 42 X. Liu, Y. Li, W. Zhu and P. Fu, *CrystEngComm*, 2013, **15**, 4937.
- 43 J. B. Fei, Y. Cui, X. H. Yan, W. Qi, Y. Yang, K. W. Wang, Q. He and J. B. Li, *Adv. Mater.*, 2008, **20**, 452.
- 44 Z. Zhang, Q. Li, S. Jiang, K. Zhang, Y. Lai and J. Li, *Chem. – Eur. J.*, 2015, **21**, 1343.
- 45 X. F. Yang, J. H. Yang, Y. L. Zhong, V. Gariepy, M. L. Trudeau, K. Zaghbi and J. Y. Ying, *ChemSusChem*, 2014, **7**, 1618.
- 46 Y. Choi, S. Hong, L. Liu, S. K. Kim and S. Park, *Langmuir*, 2012, **28**, 6670.
- 47 P. Li, H. Fan, Y. Cai and M. Xu, *CrystEngComm*, 2014, **16**, 2715.
- 48 H. Lv, Q. Lin, K. Zhang, K. Yu, T. Yao, X. Zhang, J. Zhang and B. Yang, *Langmuir*, 2008, **24**, 13736.
- 49 M. Yang, Q. Cai, C. Liu, R. Wu, D. Sun, Y. Chen, Y. Tang and T. Lu, *J. Mater. Chem. A*, 2014, **2**, 13738.
- 50 X. Liu, H. Yang, L. Han, W. Liu, C. Zhang, X. Zhang, S. Wang and Y. Yang, *CrystEngComm*, 2013, **15**, 7769.
- 51 B. Wang, G. Wang and H. Wang, *Electrochim. Acta*, 2015, **156**, 1.
- 52 D. Dorfs, H. Henschel, J. Kolny and A. Eychemüller, *J. Phys. Chem. C*, 2013, **117**, 23385.
- 53 S. H. Hwang, J. Yun and J. Jang, *Adv. Funct. Mater.*, 2014, **24**, 7619.
- 54 G. Liua, G. Hongb, X. Donga and J. Wangc, *J. Rare Earths*, 2007, **25**, 407.
- 55 J. Gu, S. Li, M. Ju and E. Wang, *J. Cryst. Growth*, 2011, **320**, 46.
- 56 G. Jia, H. G. You, Y. Song, Y. Huang, M. Yang and H. Zhang, *Inorg. Chem.*, 2010, **49**, 7721.
- 57 Z. Yang, Z. Niu, Y. Lu, Z. Hu and C. C. Han, *Angew. Chem., Int. Ed.*, 2003, **115**, 1987.
- 58 H. Lee, J.-A. Kwak and D.-J. Jang, *J. Phys. Chem. C*, 2014, **118**, 22792.
- 59 H. Zhang, C. Xu, P. Sheng, Y. Chen, L. Yu and Q. Lia, *Sens. Actuators, B*, 2013, **181**, 99.
- 60 M. Zhao, L. Zheng, X. Bai, N. Li and L. Yu, *Colloids Surf., A*, 2009, **346**, 229.
- 61 M. D. Kim, S. A. Dergunov and E. Pinkhassik, *Langmuir*, 2015, **31**, 2561.
- 62 J. Liu, S. Z. Qiao, J. S. Chen, X. W. Lou, X. Xing and G. Q. Lu, *Chem. Commun.*, 2011, **47**, 12578.
- 63 C. Liu, J. Li, J. Qi, J. Wang, R. Luo, J. Shen, X. Sun, W. Han and L. Wang, *ACS Appl. Mater. Interfaces*, 2014, **6**, 13167.
- 64 M. Kim, J. C. Park, A. Kim, K. H. Park and H. Song, *Langmuir*, 2012, **28**, 6441.
- 65 S. Wu, J. Kaiser, M. Drechsler, M. Ballauff and Y. Lu, *Colloid Polym. Sci.*, 2013, **291**, 231.
- 66 J. Liu, H. Q. Yang, F. Kleitz, Z. G. Chen, T. Yang, E. Strounina, G. Q. Lu and S. Z. Qiao, *Adv. Funct. Mater.*, 2012, **22**, 591.
- 67 Z. Zhang, F. Xiao, J. Xi, T. Sun, S. Xiao, H. Wang, S. Wang and Y. Liu, *Sci. Rep.*, 2014, **4**, 4053.
- 68 J. Lee, J. C. Park and H. Song, *Adv. Mater.*, 2008, **20**, 1523.
- 69 G. L. Li, Q. Shi, S. J. Yuan, K. G. Neoh, E. T. Kang and X. L. Yang, *Chem. Mater.*, 2010, **22**, 1309.
- 70 K. Zhang, X. H. Zhang, H. T. Chen, X. Chen, L. L. Zheng, J. H. Zhang and B. Yang, *Langmuir*, 2004, **20**, 11312.
- 71 X. W. Lou and L. A. Archer, *Adv. Mater.*, 2008, **20**, 1853.
- 72 P. Valle-Vigó n, M. Sevilla and A. B. Fuertes, *Mater. Lett.*, 2010, **64**, 1587.
- 73 L. Kong, G. T. Duan, G. M. Zuo, W. P. Cai and Z. X. Cheng, *Mater. Chem. Phys.*, 2010, **123**, 421.
- 74 N. Zhou, L. Polavarapu, Q. Wang and Q.-H. Xu, *ACS Appl. Mater. Interfaces*, 2015, **7**, 4844.
- 75 Q. H. Yang, D. F. Han, H. Q. Yang and C. Li, *Chem. – Asian J.*, 2008, **3**, 1214.
- 76 L. Li, F. G. Tang, H. Liu, T. Liu, N. Hao, D. Chen, X. Teng and J. He, *ACS Nano*, 2010, **4**, 6874.
- 77 W. Zhang, Y. Wang, X. Sun, W. Wang and L. Chen, *Nanoscale*, 2014, **6**, 14514.
- 78 H. Liu, T. Liu, X. Wu, L. Li, L. Tan, D. Chen and F. Tang, *Adv. Mater.*, 2012, **24**, 755.
- 79 J. Lim, J. H. Um, J. Ahn, S.-H. Yu, Y.-E. Sung and J.-K. Lee, *Chem. – Eur. J.*, 2015, **21**, 7954.
- 80 W. M. Zhang, J.-S. Hu, Y. G. Guo, S. F. Zheng, L. S. Zhong, W. G. Song and L. J. Wan, *Adv. Mater.*, 2008, **20**, 1160.
- 81 E. A. Khan, E. Hu and Z. Lai, *Microporous Mesoporous Mater.*, 2009, **118**, 210.
- 82 S. Kandula and P. Jeevanandam, *Eur. J. Inorg. Chem.*, 2015, 4260.
- 83 Y.-C. Yang, H.-J. Wang, J. Whang, J.-S. Huang, L.-M. Lyu, P.-H. Lin, S. Gwo and M. H. Huang, *Nanoscale*, 2014, **6**, 4316.
- 84 K. K. Haldar, S. Kundu and A. Patra, *ACS Appl. Mater. Interfaces*, 2014, **6**, 21946.
- 85 J. Tian, Y. Luo, H. Li, W. Lu, G. Chang, X. Qin and X. Sun, *Catal. Sci. Technol.*, 2011, **1**, 1393.
- 86 W. Jiang, Y. Zhou, Y. Zhang, S. Xuan and X. Gong, *Dalton Trans.*, 2012, **41**, 4594.
- 87 N. Rinaldi-Montes, P. Gorria, D. Martínez-Blanco, Z. Amghouz, A. B. Fuertes, L. F. Barquín, I. de Pedro, L. Olivi and J. A. Blanco, *J. Mater. Chem. C*, 2015, **3**, 5674.
- 88 L. Zhang, P. Hu, X. Zhao, R. Tian, R. Zou and D. Xia, *J. Mater. Chem.*, 2011, **21**, 18279.
- 89 M. Abdul Matin, E. Lee, H. Kim, W.-S. Yoon and Y.-Uk Kwon, *J. Mater. Chem. A*, 2015, **3**, 17154.
- 90 K. S. Kumar, V. B. Kumar and P. Paik, *Chem. Commun.*, 2011, **47**, 6837.
- 91 J. Tian, J. Jin, F. Zheng and H. Zhao, *Langmuir*, 2010, **26**, 8762.
- 92 X. Xue, F. Wang and X. Liu, *J. Mater. Chem.*, 2011, **21**, 13107.
- 93 J. Kim, Y. Piao and T. Hyeon, *Chem. Soc. Rev.*, 2009, **38**, 372.

- 94 Y. W. Jun, J. H. Lee and J. Cheon, *Angew. Chem., Int. Ed.*, 2008, **47**, 5122.
- 95 Y. Li, Y. C. Liu, J. Tang, H. Q. Lin, N. Yao, X. Z. Shen, C. H. Deng, P. Y. Yang and X. M. Zhang, *J. Chromatogr. A*, 2007, **1172**, 57.
- 96 Y. Li, T. H. Leng, H. Q. Lin, C. H. Deng, X. Q. Xu, N. Yao, P. Y. Yang and X. M. Zhang, *J. Proteome Res.*, 2007, **6**, 4498.
- 97 Y. Li, X. Q. Xu, D. W. Qi, C. H. Deng, P. Y. Yang and X. M. Zhang, *J. Proteome Res.*, 2008, **7**, 2526.
- 98 D. Delaportas, P. Svarnas, I. Alexandrou, S. N. Georga, C. A. Krontiras, N. I. Xanthopoulos, A. Siokou and P. R. Chalker, *Mater. Lett.*, 2011, **65**, 2337.
- 99 X. Zhu, L. Wu, D. C. Mungra, S. Xia and J. Zhu, *Analyst*, 2012, **137**, 2454.
- 100 Z. Bai, R. Chen, P. Si, Y. Huang, H. Sun and D.-H. Kim, *ACS Appl. Mater. Interfaces*, 2013, **5**, 5856.
- 101 Y. Hu, K. Tao, C. Wu, C. Zhou, H. Yin and S. Zhou, *J. Phys. Chem. C*, 2013, **117**, 7.
- 102 Z. W. Seh, S. Liu, S.-Y. Zhang, K. W. Shah and M.-Y. Han, *Chem. Commun.*, 2011, **47**, 6689.
- 103 L. D. Rogatis, M. Cargnello, V. Gombac, B. Lorenzut, T. Montini and P. Fornasiero, *ChemSusChem*, 2010, **3**, 24.
- 104 N. L. Wieder, M. Cargnello, K. Bakhmutsky, T. Montini, P. Fornasiero and R. J. Gorte, *J. Phys. Chem. C*, 2011, **115**, 915.
- 105 Z. Zhuang, Q. Peng and Y. Li, *Chem. Soc. Rev.*, 2011, **40**, 5492.
- 106 N. Zhang, X. Fu and Y.-J. Xu, *J. Mater. Chem.*, 2011, **21**, 8152.
- 107 G. Li and Z. Tang, *Nanoscale*, 2014, **6**, 3995.
- 108 J. Lin, W. Zhou, A. Kumbhar, J. Wiemann, J. Fang, E. E. Carpenter and C. J. O'Connor, *J. Solid State Chem.*, 2001, **159**, 26.
- 109 E. E. Carpenter, J. A. Sims, J. A. Wienmann, W. L. Zhou and C. J. O'Connor, *J. Appl. Phys.*, 2000, **87**, 5615.
- 110 G. Salazar-Alvarez, M. Mikhailova, M. Toprak, Y. Zhang and M. Muhammed, *Mater. Res. Soc. Symp. Proc.*, 2001, **707**, 263.
- 111 D. A. Fleming, M. Napolitano and M. E. Williams, *Mater. Res. Soc. Symp. Proc.*, 2003, **746**, 207.
- 112 S. U. Son, Y. Jang, J. Park, H. B. Na, H. M. Park, H. J. Yun, J. Lee and T. Hyeon, *J. Am. Chem. Soc.*, 2004, **126**, 5026.
- 113 Z. Xu, Y. Hou and S. Sun, *J. Am. Chem. Soc.*, 2007, **129**, 8698.
- 114 G. Büchel, K. K. Unger, A. Matsumoto and K. Tsutsumi, *Adv. Mater.*, 1998, **10**, 1036.
- 115 Y. Deng, D. Qi, C. Deng, X. Zhang and D. Zhao, *J. Am. Chem. Soc.*, 2008, **130**, 28.
- 116 A. M. El-Toni, M. W. Khan, M. A. Ibrahim, M. Abid, M. Al-Hoshan and M. Al-salhi, *Chem. Commun.*, 2010, **46**, 6482.
- 117 A. M. El-Toni, M. A. Ibrahim, J. P. Labis, A. Khan and M. Alhoshan, *Int. J. Mol. Sci.*, 2013, **14**, 11496.
- 118 X. Qian, J. Du, B. Li, M. Si, Y. Yang, Y. Hu, G. Niu, Y. Zhang, H. Xu, B. Tu, Y. Tang and D. Zhao, *Chem. Sci.*, 2011, **2**, 2006.
- 119 J. Ge, Q. Zhang, T. Zhang and Y. Yin, *Angew. Chem., Int. Ed.*, 2008, **47**, 8924.
- 120 Z. Zhong, Y. Yin, B. Gates and Y. Xia, *Adv. Mater.*, 2000, **12**, 206.
- 121 Y. Chen, E. T. Kang, K. G. Neoh and A. Greiner, *Adv. Funct. Mater.*, 2005, **15**, 113.
- 122 Y. Wang, Q. Zhu and H. Zhang, *Chem. Commun.*, 2005, 5231.
- 123 L. Zhen and W. Shu-Bin, *J. Inorg. Mater.*, 2011, **26**, 885.
- 124 A. Syoufian, Y. Inoue, A. Yada and K. Nakashima, *Mater. Lett.*, 2007, **61**, 1572.
- 125 J.-S. Jan, T.-H. Chuang, P.-J. Chen and H. Teng, *Langmuir*, 2011, **27**, 2834.
- 126 F. Caruso, R. A. Caruso and H. Möhwald, *Science*, 1998, **282**, 1111.
- 127 L. Wang, Y. Ebina, K. Takada and T. Sasaki, *Chem. Commun.*, 2004, 1074.
- 128 F. Caruso, X. Shi, R. A. Caruso and A. Susha, *Adv. Mater.*, 2001, **13**, 740.
- 129 N. Wang, Y. Gao, J. Gong, X. Ma, X. Zhang, Y. Guo and L. Qu, *Eur. J. Inorg. Chem.*, 2008, 3827.
- 130 Y. Liu, P. Yang, W. Wang, H. Donga and J. Lin, *CrystEngComm*, 2010, **12**, 3717.
- 131 M. Titirici, M. Antonietti and A. Thomas, *Chem. Mater.*, 2006, **18**, 3808.
- 132 L. Shen, L. Yu, X.-Y. Yu, X. Zhang and X. W. Lou, *Angew. Chem., Int. Ed.*, 2015, **54**, 1868.
- 133 J. H. Pan, Y. Bai and Q. Wang, *Langmuir*, 2015, **31**, 4566.
- 134 J. H. Pan, C. Shen, I. Ivanova, N. Zhou, X. Wang, W. C. Tan, Q.-H. Xu, D. W. Bahnemann and Q. Wang, *ACS Appl. Mater. Interfaces*, 2015, **7**, 14859.
- 135 H. Xu and W. Wang, *Angew. Chem., Int. Ed.*, 2007, **46**, 1489.
- 136 M. Sasidharan and K. Nakashima, *Acc. Chem. Res.*, 2014, **47**, 157.
- 137 P. Leidinger, R. Popescu, D. Gerthsen and C. Feldmann, *Small*, 2010, **6**, 1886.
- 138 Y. Sun, Y. Liu, G. Zhao and Q. Zhang, *Nanoscale Res. Lett.*, 2008, **3**, 82.
- 139 L. Li, E. S. Choo, X. Tang, J. Ding and J. Xue, *Chem. Commun.*, 2009, 938.
- 140 C. I. Zoldesi, C. A. van Walree and A. Imhof, *Langmuir*, 2006, **22**, 4343.
- 141 L. Y. Li, D. B. Qin, X. L. Yang and G. Y. Liu, *Polym. Chem.*, 2010, **1**, 289.
- 142 H. Zhang and X. L. Yang, *Polym. Chem.*, 2010, **1**, 670.
- 143 X. W. Lou, C. Yuan and L. A. Archer, *Small*, 2007, **3**, 261.
- 144 D. Chen, L. L. Li, F. Q. Tang and S. Qi, *Adv. Mater.*, 2009, **21**, 3804.
- 145 Y. F. Zhu, E. Kockrick, T. Ikoma, N. Hanagata and S. Kaskel, *Chem. Mater.*, 2009, **21**, 2547.
- 146 J. Yang, D. Shen, L. Zhou, W. Li, J. Fan, A. M. El-Toni, W.-X. Zhang, F. Zhang and D. Zhao, *Adv. Healthcare Mater.*, 2014, **3**, 1620.
- 147 J. Yang, D. Shen, L. Zhou, W. Li, X. Li, C. Yao, R. Wang, A. M. El-Toni, F. Zhang and D. Zhao, *Chem. Mater.*, 2013, **25**, 3030.

- 148 T. R. Zhang, J. P. Ge, Y. X. Hu, Q. Zhang, S. Aloni and Y. D. Yin, *Angew. Chem., Int. Ed.*, 2008, **47**, 5806.
- 149 Q. Zhang, J. P. Ge, J. Goebel, Y. X. Hu, Z. D. Lu and Y. D. Yin, *Nano Res.*, 2009, **2**, 583.
- 150 A. Popat, S. B. Hartono, F. Stahr, J. Liu, S. Z. Qiao and G. Q. M. Lu, *Nanoscale*, 2011, **7**, 2801.
- 151 L. Zhang, S. Z. Qiao, Y. G. Jin, Z. G. Chen, H. C. Gu and G. Q. M. Lu, *Adv. Mater.*, 2008, **20**, 805.
- 152 X. J. Wu and D. S. Xu, *J. Am. Chem. Soc.*, 2009, **131**, 2774.
- 153 S. N. Shmakov, Y. Jia and E. Pinkhassik, *Chem. Mater.*, 2014, **26**, 1126.
- 154 Z.-A. Qiao, Q. Huo, M. Chi, G. M. Veith, A. J. Binder and S. Dai, *Adv. Mater.*, 2012, **24**, 6017.
- 155 J. Han, M. Wang, R. Chen, N. Han and R. Guo, *Chem. Commun.*, 2014, **50**, 8295.
- 156 S. J. Ding, J. S. Chen, G. G. Qi, X. N. Duan, Z. Y. Wang, E. P. Giannelis, L. A. Archer and X. W. Lou, *J. Am. Chem. Soc.*, 2011, **133**, 21.
- 157 L. M. Guo, X. Z. Cui, Y. S. Li, Q. J. He, L. X. Zhang, W. B. Bu and J. L. Shi, *Chem. – Asian J.*, 2009, **4**, 1480.
- 158 H. C. Zeng, *Curr. Nanosci.*, 2007, **3**, 177.
- 159 X. Wang, Y. Wanga, L. Yanga, K. Wang, X. Lou and B. Cai, *J. Power Sources*, 2014, **262**, 72.
- 160 X. Tian, J. Li, K. Chen, J. Han and S. Pan, *Cryst. Growth Des.*, 2009, **9**, 4927.
- 161 B. Liu and H. C. Zeng, *Small*, 2005, **1**, 566.
- 162 H. Gao, G. Wang, Y. Luan, K. Chaikittikul, X. Zhang, M. Yang, W. Dong and Z. Shi, *CrystEngComm*, 2014, **16**, 2520.
- 163 S. Xie, M. Jin, J. Tao, Y. Wang, Z. Xie, Y. Zhu and Y. Xia, *Chem. – Eur. J.*, 2014, **18**, 14974.
- 164 H. Jang and D.-H. Min, *ACS Nano*, 2015, **9**, 2696.
- 165 Q. Shi, P. Zhang, Y. Li, H. Xia, D. Wang and X. Tao, *Chem. Sci.*, 2015, **6**, 4350.
- 166 L. Zhou, J. Yuan and Y. Wei, *J. Mater. Chem.*, 2011, **21**, 2823.
- 167 S. Cheong, P. Ferguson, I. F. Hermans, G. N. L. Jameson, S. Prabakar, D. A. J. Herman and R. D. Tilley, *Chem-PlusChem*, 2012, **77**, 135.
- 168 S. Laurent, D. Forge, M. Port, A. Roch, C. Robic, L. V. Elst and R. N. Muller, *Chem. Rev.*, 2008, **108**, 2064.
- 169 N. Sounderya and Y. Zhang, *Recent Pat. Biomed. Eng.*, 2008, **1**, 34.
- 170 W. Schärfl, *Adv. Mater.*, 2000, **12**, 1899.
- 171 V. Salgueiri~no-Maceira and M. Correa-Duarte, *Adv. Mater.*, 2007, **19**, 4131.
- 172 D. Knopp, D. Tang and R. Niessner, *Anal. Chim. Acta*, 2009, **647**, 14.
- 173 M. De, P. S. Ghosh and V. M. Rotello, *Adv. Mater.*, 2008, **20**, 4225.
- 174 W. Schärfl, *Nanoscale*, 2010, **2**, 829.
- 175 G. Wang and A. J. Harrison, *Colloid Interface Sci.*, 1999, **217**, 203.
- 176 S. Deng, K. C. Pinagali and D. A. Rockstraw, *IEEE Sens. J.*, 2008, **8**, 730.
- 177 Y. H. Lien and T. M. Wu, *J. Colloid Interface Sci.*, 2008, **326**, 517.
- 178 S. Santra, R. Tapeç, N. Theodoropoulou, J. Dobson, A. Hebard and W. Tan, *Langmuir*, 2001, **17**, 2900.
- 179 W. R. Lee, M. G. Kim, J. R. Choi, J.-I. Park, S. J. Ko, S. J. Oh and J. Cheon, *J. Am. Chem. Soc.*, 2005, **127**, 16090.
- 180 B. Chertok, A. E. David and V. C. Yang, *Biomaterials*, 2010, **31**, 6317.
- 181 C. Pathak, Y. K. Jaiswal and M. Vinayak, *Biosci. Rep.*, 2008, **28**, 73.
- 182 M. F. Kircher, U. Mahmood, R. S. King, R. Weissleder and L. Josephson, *Cancer Res.*, 2003, **63**, 8122.
- 183 W. Tan, K. Wang, X. He, X. J. Zhao, T. Drake, L. Wang and R. P. Bagwe, *Med. Res. Rev.*, 2004, **24**, 621.
- 184 E. A. Schellenberger, D. Sosnovik, R. Weissleder and L. Josephson, *Bioconjugate Chem.*, 2004, **15**, 1062.
- 185 H. Daneshvar, J. Nelms, O. Muhammad, H. Jackson, J. Tkach, W. Davros, T. Peterson, M. A. Vogelbaum, M. P. Bruchez and S. A. Toms, *Nanomedicine*, 2008, **3**, 21.
- 186 A. SalmanOgli and A. J. Rostami, *Nanopart. Res.*, 2010, **13**, 1197.
- 187 W. Wu, T. Zhou, A. Berliner, P. Banerjee and S. Zhou, *Chem. Mater.*, 2010, **22**, 1966.
- 188 Y. Wang, Z. Tang, M. A. Correa-Duarte, I. Pastoriza-Santos, M. Giersig, N. A. Kotov and L. M. Liz-Marzan, *J. Phys. Chem. B*, 2004, **108**, 15461.
- 189 Y. Wang, L. Tu, J. Zhao, Y. Sun, X. Kong and H. Zhang, *J. Phys. Chem. C*, 2009, **113**, 7164.
- 190 H. S. Qian and Y. Zhang, *Langmuir*, 2008, **24**, 12123.
- 191 L. Stanciu, Y.-H. Won, M. Ganesana and S. Andreescu, *Sensors*, 2009, **9**, 2976.
- 192 J. D. Qiu, S. G. Cui, M. Q. Deng and R. P. Liang, *J. Appl. Electrochem.*, 2010, **40**, 1651.
- 193 J. D. Qiu, S. G. Cui and R. P. Liang, *Microchim. Acta*, 2010, **171**, 333.
- 194 B. Dong, L. Cao, G. Su, W. Liu, H. Qu and D. Jiang, *J. Colloid Interface Sci.*, 2009, **339**, 78.
- 195 N. Khlebtsov, V. Bogatyrev, L. Dykman, B. Khlebtsov, S. Staroverov, A. Shirokov, L. Matora, V. Khanadeev, T. Pylaev, N. Tsyganova and G. Terentyuk, *Theranostics*, 2013, **3**, 167.
- 196 X. Wang, T. Yang and K. Jiao, *Biosens. Bioelectron.*, 2009, **25**, 668.
- 197 J. D. Qiu, H. P. Peng, R. P. Liang and X. H. Xia, *Biosens. Bioelectron.*, 2010, **25**, 1447.
- 198 X. F. Zhang, X. L. Dong, H. Huang, B. Lv, X. G. Zhu, J. P. Lei, S. Ma, W. Liu and Z. D. Zhang, *Mater. Sci. Eng., A*, 2007, **454–455**, 211.
- 199 H. Yin, Z. Ma, M. Chi and S. Dai, *Catal. Today*, 2011, **160**, 87.
- 200 S. Xuan, Y. X. J. Wang, J. C. Yu and K. C. F. Leung, *Langmuir*, 2009, **25**, 11835.
- 201 C. L. Carnes and K. J. Klabunde, *Chem. Mater.*, 2002, **14**, 1806.
- 202 J. J. Schneider, *Adv. Mater.*, 2001, **3**, 529.
- 203 L. H. Yao, Y. X. Li, J. Zhao, W. J. Ji and C. T. Au, *Catal. Today*, 2010, **158**, 401.

- 204 R. Ferrando, J. Jellinek and R. L. Johnston, *Chem. Rev.*, 2008, **108**, 845.
- 205 D. Xiong, Z. Li, Y. An, R. Ma and L. Shi, *J. Colloid Interface Sci.*, 2010, **350**, 260.
- 206 L. Wang and Y. J. Yamauchi, *Am. Chem. Soc.*, 2010, **132**, 13636.
- 207 D. Zhao, X. Chen, Y. Liu, C. Wu, R. Ma, Y. An and L. Hi, *J. Colloid Interface Sci.*, 2009, **331**, 104.
- 208 L. Feng, G. Gao, P. Huang, K. Wang, X. Wang, T. Luo and C. Zhang, *Nano Biomed. Eng.*, 2010, **2**, 258.
- 209 F.-R. Fan, D.-Y. Liu, Y.-F. Wu, S. Duan, Z.-X. Xie, Z.-Y. Jiang and Z.-Q. Tian, *J. Am. Chem. Soc.*, 2008, **130**, 6949.
- 210 Y. Zhao, Y. Ding, Y. Li, L. Peng, H. R. G. Byon, J. B. Goodenough and G. Yu, *Chem. Soc. Rev.*, 2015, **44**, 7968.
- 211 C. Z. Wu, Y. Xie, L. Y. Lei, S. Q. Hu and C. Z. OuYang, *Adv. Mater.*, 2006, **18**, 1727.
- 212 C.-M. Park, J.-H. Kim, H. Kim and H.-J. Sohn, *Chem. Soc. Rev.*, 2010, **39**, 3115.
- 213 M. Winter, J. O. Besenhard, M. E. Spahr and P. Novak, *Adv. Mater.*, 1998, **10**, 725.
- 214 P. Poizot, S. Laruelle, S. Grugeon, L. Dupont and J. M. Tarascon, *Nature*, 2000, **407**, 496.
- 215 X. Wang, Z. Li, Z. Zhang, Q. Li, E. Guo, C. Wang and L. Yin, *Nanoscale*, 2015, **7**, 3604.
- 216 F. Wu, Z. Wang, Y. Su, Y. Guan, Y. Jin, N. Yan, J. Tian, L. Bao and S. Chen, *J. Power Sources*, 2014, **267**, 337.
- 217 S. W. Kim, M. Kim, W. Y. Lee and T. Hyeon, *J. Am. Chem. Soc.*, 2002, **124**, 7642.
- 218 Y. G. Li, P. Zhou, Z. H. Dai, Z. X. Hu, P. P. Sun and J. C. Bao, *New J. Chem.*, 2006, **30**, 832.
- 219 F. Y. Cheng, H. Ma, Y. M. Li and J. Chen, *Inorg. Chem.*, 2007, **46**, 788.
- 220 X.-C. Zhou, X.-H. Zhu, J.-W. Huang, X.-Z. Li, P.-F. Fu, L.-X. Jiao, H.-F. Huo and R. Li, *RSC Adv.*, 2014, **4**, 33055.
- 221 Y. Jiao, F. Wang, X. Ma, Q. Tang, K. Wang, Y. Guo and L. Yang, *Microporous Mesoporous Mater.*, 2013, **176**, 1.
- 222 Q. Zhang, T. Wu, P. Zhang, R. Qi, R. Huang, X. Song and L. Gao, *RSC Adv.*, 2014, **4**, 51184.
- 223 H. P. Liang, H. M. Zhang, J. S. Hu, Y. G. Guo, L. J. Wan and C. L. Bai, *Angew. Chem., Int. Ed.*, 2004, **43**, 1540.
- 224 Y.-B. Cho, J. E. Kim, J. H. Shim, C. Lee and Y. Lee, *Phys. Chem. Chem. Phys.*, 2013, **15**, 11461.
- 225 J. Sun, J. Zhang, M. Zhang, M. Antonietti, X. Fu and X. Wang, *Nat. Commun.*, 2012, **3**, 1139.
- 226 Y. Zheng, L. Lin, B. Wang and X. Wang, *Angew. Chem., Int. Ed.*, 2015, **54**, 12868.
- 227 D. Zheng, C. Huang and X. Wang, *Nanoscale*, 2015, **7**, 465.
- 228 D. Zheng, C. Pang, Y. Liu and X. Wang, *Chem. Commun.*, 2015, **51**, 9706.
- 229 D. Zheng, G. Zhang and X. Wang, *Appl. Catal., B*, 2015, **179**, 479.
- 230 D. Zheng, C. Pang and X. Wang, *Chem. Commun.*, 2015, **51**, 17467.
- 231 N. T. K. Thanh, *Nanoscale*, 2013, **5**, 11338.
- 232 Z. P. Xu, T. L. Walker, K.-L. Liu, H. M. Cooper, G. M. Lu and P. F. Bartlett, *Int. J. Nanomed.*, 2007, **2**, 163.
- 233 J. Guo, M. J. Armstrong, C. M. O'Driscoll, J. D. Holmes and K. Rahme, *RSC Adv.*, 2015, **5**, 17862.
- 234 J. F. Chen, H. M. Ding, J. X. Wang and L. Shao, *Biomaterials*, 2004, **25**, 723.
- 235 Z. Z. Li, L. X. Wen, L. Shao and J. F. Chen, *J. Controlled Release*, 2004, **98**, 245.
- 236 N. E. Botterhuis, Q. Y. Sun, P. C. M. M. Magusin, R. A. van Santen and N. A. J. M. Sommerdijk, *Chem. – Eur. J.*, 2006, **12**, 1448.
- 237 J. Zhou, W. Wu, D. Caruntu, M. H. Yu, A. Martin, J. F. Chen, C. J. O'Connor and W. L. Zhou, *J. Phys. Chem. C*, 2007, **111**, 17473.
- 238 V. V. Sokolova, I. Radtke, R. Heumann and M. Epple, *Biomaterials*, 2006, **27**, 3147.
- 239 Y. R. Cai, H. H. Pan, X. R. Xu, Q. H. Hu, L. Li and R. K. Tang, *Chem. Mater.*, 2007, **19**, 3081.
- 240 J. Chen, F. Saeki, B. J. Wiley, H. Cang, M. J. Cobb, Z. Y. Li, L. Au, H. Zhang, M. B. Kimmey, X. D. Li and Y. Xia, *Nano Lett.*, 2005, **5**, 473.
- 241 S. Skrabalak, J. Chen, L. Au, X. Lu, X. Li and Y. Xia, *Adv. Mater.*, 2007, **19**, 3177.
- 242 J. Y. Chen, D. L. Wang, J. F. Xi, L. Au, A. Siekkinen, A. Warsen, Z. Y. Li, H. Zhang, Y. N. Xia and X. D. Li, *Nano Lett.*, 2007, **7**, 1318.
- 243 D. M. Vriezema, M. C. Aragonés, J. A. A. W. Elemans, J. J. L. M. Cornelissen, A. E. Rowan and R. J. M. Nolte, *Chem. Rev.*, 2005, **105**, 1445.
- 244 J. Lee, J. C. Park, J. U. Bang and H. Song, *Chem. Mater.*, 2008, **20**, 5839.
- 245 Y. Yang, W. Zhang, Y. Zhang, A. Zheng, H. Sun, X. Li, S. Liu, P. Zhang and X. Zhang, *Nano Res.*, 2015, **8**, 3404.
- 246 L. Yang, M. C. Zhang, Y. Lan and W. Q. Zhang, *New J. Chem.*, 2010, **34**, 1355.
- 247 B. Guan, T. Wang, S. Zeng, X. Wang, D. An, D. Wang, Y. Cao, D. Ma, Y. Liu and Q. Huo, *Nano Res.*, 2013, **7**, 246.
- 248 C.-H. Lin, X. Liu, S.-H. Wu, K.-H. Liu and C.-Y. Mou, *J. Phys. Chem. Lett.*, 2011, **2**, 2984.
- 249 Z. Li, L. Mo, Y. Kathiraser and S. Kawi, *ACS Catal.*, 2014, **4**, 1526.
- 250 J. Jiang, S.-H. Kim and L. Piao, *Nanoscale*, 2015, **7**, 8299.
- 251 Z. Chen, Z. M. Cui, F. Niu, L. Jiang and W. G. Song, *Chem. Commun.*, 2010, **46**, 6524.
- 252 H. J. Hah, J. I. Um, S. H. Han and S. M. Koo, *Chem. Commun.*, 2004, 1012.
- 253 Y. Xia and L. Xu, *Synth. Met.*, 2010, **160**, 545.
- 254 Z. Zhang, F. Xiao, J. Xi, T. Sun, S. Xiao, H. Wang, S. Wang and Y. Liu, *Sci. Rep.*, 2014, **4**, 4053.
- 255 R. J. Dillon, J. B. Joo, F. Zaera, Y. Yin and C. J. Bardeen, *Phys. Chem. Chem. Phys.*, 2013, **15**, 1488.
- 256 H. X. Li, Z. F. Bian, J. Zhu, Y. N. Huo, H. Li and Y. F. Lu, *J. Am. Chem. Soc.*, 2007, **129**, 8406.

- 257 M. Wang, J. Han, H. Xiong and R. Guo, *Langmuir*, 2015, **31**, 6220.
- 258 W. Su, T. Zhang, L. Li, J. Xing, M. He, Y. Zhong and Z. Li, *RSC Adv.*, 2014, **4**, 8901.
- 259 C.-M. Huang, S.-H. Cheng, U.-S. Jeng, C.-S. Yang and L.-W. Lo, *Nano Res.*, 2012, **5**, 654.
- 260 Y. Wang, G. Wang, Y. Xiao, Y. Yang and R. Tang, *ACS Appl. Mater. Interfaces*, 2014, **6**, 19092.
- 261 W. R. Zhao, H. R. Chen, Y. S. Li, L. Li, M. D. Lang and J. L. Shi, *Adv. Funct. Mater.*, 2008, **18**, 2780.
- 262 P. Du and P. Liu, *Langmuir*, 2014, **30**, 3060.
- 263 H. Chen, B. Qi, T. Moore, F. Wang, D. C. Colvin, L. D. Sanjeeva, J. C. Gore, S.-J. Hwu, O. T. Mefford, F. Alexis and J. N. Anker, *Small*, 2014, **10**, 3364.
- 264 X. F. Zhang, L. Clime, H. Q. Ly, M. Trudeau and T. Veres, *J. Phys. Chem. C*, 2010, **114**, 18313.